**FIGURE 5.** Prevention of experimental asthma by the transfer of CD4$^+$ cells and CD11c$^+$ spleen cells from high-dose OVA-fed mice. Naive BALB/c mice were immunized as described for Fig. 1. A total of 10$^7$ CD4$^+$ cells or 10$^6$ CD11c$^+$ spleen cells of OVA-fed mice were adoptively transferred by i.v. injection into naive BALB/c mice just before the first immunization with OVA in aluminum hydroxide (Fed/CD4$^+$ or Fed/CD11c$^+$ transfer). The control mice were injected with whole spleen cells of water-fed mice (Non-fed/Whole transfer) or OVA-fed (Fed/Whole transfer) mice. At 24 h after the final inhalation (day 21), airway hyperresponsiveness was measured. After the measurement of airway hyperresponsiveness, BALF and blood samples were obtained and the whole lung was removed for histological examination. *A*, The percentage of eosinophils in BALF. The cell differentials in the BALF were identified by morphologic criteria. *B*, Airway hyperresponsiveness was assessed by methacholine-induced airflow obstruction. Airway hyperresponsiveness was expressed as PC$_{200}$Mch. *C*, The levels of serum OVA-specific IgE, OVA-specific IgG1, and OVA-specific IgG2a were assayed by ELISA. *D*, Histological examination of the lung tissue. Histological findings were evaluated and scored into four grades based on the distribution and intensity of inflammation as described in *Materials and Methods*. Representative histological findings in lungs were stained with H&E or PAS. Magnification ×100 with H&E stain (*a*), ×200 with H&E (*e*), and ×200 with PAS (*i*) of lung tissue from Non-fed/Whole transfer mice. Magnification ×100 with H&E stain (*b*), ×200 with H&E (*f*), and × 200 with PAS (*j*) of lung tissue from Fed/Whole transfer mice. Magnification ×100 with H&E stain (*c*), ×200 with H&E (*g*), and ×200 with PAS (*k*) of lung tissue from Fed/CD4$^+$ transfer mice. Magnification ×100 H&E stain (*d*), ×200 with H&E (*h*), and ×200 with PAS (*l*) of lung tissue from Fed/CD11c$^+$ transfer mice. Mucus production is stained red with PAS. Statistically significant data (*) are indicated.
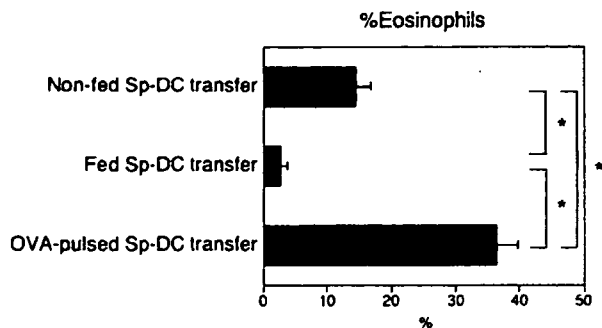
**FIGURE 6.** Comparison of the effects of in vivo and in vitro Ag loading upon the transfer of oral tolerance. Naive BALB/c mice were immunized as described in Fig. 1. A total of $10^6$ CD11c$^+$ spleen cells of water-fed mice (Non-fed Sp-DC transfer). $10^6$ CD11c$^{-1}$ spleen cells of OVA-fed mice (Fed Sp-DC transfer), or $10^6$ CD11c$^+$ spleen cells of naive BALB/c mice that were pulsed with OVA in vitro (OVA-pulsed Sp-DC transfer) were adoptively transferred by i.v. injection into naive BALB/c mice just before the first immunization with OVA in aluminum hydroxide. Data are expressed as the mean percentage of eosinophils in BALF on day 21.

For clinical applications, it is important to determine whether Ag feeding exerts a suppressive effect on immune responses that are already in progress. To evaluate whether the timing of the feeding affected the induction of tolerance, we tested the animals to determine whether OVA feeding after an i.p. immunization would also prevent the disease. Our data indicated that the development of bronchial eosinophilia and airway hyperresponsiveness was not suppressed by high-dose OVA feeding just before the Ag challenge, but OVA feeding after the first immunization suppressed the development of the disease (Fig. 2). A recent report demonstrated that OVA feeding after the intranasal OVA challenge did not suppress bronchial eosinophilia, but OVA feeding after the second immunization successfully suppressed bronchial eosinophilia (12). The discrepancy between those results and ours might be due to the use of two different immunization protocols. However, it is of note that both datasets suggest the possibility of a clinical application for sensitized patients.

Oral tolerance is mediated by more than one mechanism, and the major proposed mechanisms are as follows: 1) induction of regulatory T cells secreting immunoregulatory cytokines such as TGF-$\beta$ (22) and IL-10 (26); 2) immune deviation to a Th1-type response by IFN-$\gamma$, which has been shown to inhibit the Th2-type response in vitro (27, 28) and in vivo (29–31); and 3) anergy or deletion of Ag-specific T cells (6, 18). To examine whether the suppression of bronchial eosinophilia and airway hyperresponsiveness is consistent with local cytokine and chemokine patterns in the lung, we also analyzed the gene expression of major cytokines and chemokines in whole lung tissue using RT-PCR. Th2 cytokines such as IL-4, IL-5, and IL-13 and chemokines such as eotaxin were regarded as essential mediators for the development of bronchial eosinophilia and/or airway hyperresponsiveness (32–35). Although the levels of IL-13 and eotaxin in the lung were remarkably decreased in OVA-fed mice before the first immunization (Fig. 2, D and E), the level of IL-4 or IL-5 were not suppressed as much as IL-13 (data not shown). Some reports have suggested that IL-13 is more important key regulator in the experimental airway hyperreactivity model than are IL-4 or IL-5 (36–38). Our findings suggest that the inhibition of airway hyperreactivity and eosinophilia by direct feeding of Ag was partially due to the suppression of IL-13 and eotaxin. The levels of TGF-$\beta$, IL-10, and IFN-$\gamma$ in the lung did not increase in tolerized mice, suggesting that these cytokines were not involved in the mechanism of oral tolerance in this model. Our data are in agreement with the findings of recent reports

showing that treatment with anti-TGF-$\beta$ Abs had no significant effect on the inhibition of tracheal eosinophilia (11, 12); however, the present data contradict the findings of another previous report (9) in this regard. This discrepancy could be due to the use of different immunization protocols or to the use of transgenic vs nontransgenic mice. Conversely, a recent report demonstrated that both IL-10 and TGF-$\beta$ gene expression of CD14$^+$ macrophages in BALF from Ag-fed dogs was up-regulated in a dog model of asthma, which was assessed by RT-PCR (13). However, the levels of IL-10 and TGF-$\beta$ in BALF from tolerized mice did not increase in the present series of experiments, as determined by ELISA (data not shown).

To determine whether bronchial eosinophilia in this model was actively suppressed by the cell transfer, we adoptively transferred the spleen cells of high-dose OVA-fed mice and examined whether bronchial eosinophilia was suppressed. Our data show that bronchial eosinophilia in this model was actively suppressed by whole spleen cell transfer from fed mice (Fig. 3A), even when the transfer took place during the immunization period (Fig. 3B), suggesting the possibility of a clinical application for the treatment of sensitized patients. To explore the regulatory cells in this transfer system of oral tolerance, we conducted the adoptive transfer of spleen cells depleted of specific subpopulations. Our results show that the removal of CD4$^+$ cells partially blocked active suppression (Fig. 4A), whereas the depletion of CD19$^+$ cells did not affect the transfer of tolerance (Fig. 4B). Active suppression was entirely blocked by the depletion of whole APCs or CD11b$^+$ cells, and the depletion of CD11c$^+$ cells made the bronchial eosinophilia worse than that in nontolerized mice (Fig. 4). One previous report demonstrated that the depletion of CD4$^+$ cells, but not that of CD8$^+$ cells, blocked the active suppression of pulmonary eosinophilia (9). We demonstrated in this study that the depletion of CD8$^+$ cells led only to a partial reversal of active suppression. In contrast, the depletion of CD11c$^+$ DCs blocked active suppression more effectively than did the depletion of CD4$^+$ cells. We therefore followed-up with a trial in which we purified only CD11c$^+$ cells from the spleen of OVA-fed mice and adoptively transferred them. By the transfer of CD11c$^+$ DCs, eosinophilia in BALF, airway hyperreactivity, peribronchial inflammation, and OVA-specific IgE productions were all suppressed, indicating that splenic CD11c$^+$ DCs of OVA-fed mice functioned as "regulatory cells" in the suppression of disease in this model.

Several recent studies have proposed the existence of tolerogenic or regulatory DCs (19, 39–44). Especially in the murine model of airway hyperreactivity, Akbari et al. (19, 43) have reported that the tolerance to Ag can be adoptively transferred by the pulmonary DCs exposed to respiratory Ag, which secrete IL-10. Alpan et al. (42, 44) have shown that DCs from Ag-fed animals are educated to induce regulatory T cells in vitro and that this education can be performed even by tolerized T cells. We also obtained other data showing that splenic DCs or mesenteric lymph node DCs from OVA-fed mice could transfer oral tolerance into mice immunized by OVA/CFA (Y. Tanno, K. Nagatani, and Y. Komagata, unpublished observations). In the present report, we showed that there are tolerogenic DCs not only in the lung but also in the spleen of OVA-fed mice that can transfer the tolerance to OVA in the OVA-induced murine model of asthma (Fig. 5). Mouse splenic DCs are categorized into the subpopulations of CD8$^+$CD11b$^-$CD4$^-$ DCs, CD8$^-$CD11b$^+$CD4$^-$ DCs, and CD8$^-$CD11b$^+$CD4$^+$ DCs (45). The results of the present study suggest that CD11b$^+$ DCs were more important than CD8$^+$ DCs because the depletion of CD11b$^+$ cells partially abrogated the transfer of suppression (Fig. 4B). The mechanism by which these DCs suppress airway hyperreactivity and eosinophilia in this model remains to be elucidated. Regarding the site at which these regulatory DCs are generated, it is possible that immature DCs encounter the Ags in mucosal lymphoid tissues and acquire the regulatory function. We have data showing that DCs in the dome of Peyer's patches move quickly after the capture of Ag and interact with Ag-specific T cells in the T cell

area of Peyer's patches (K. Nagatani, K. Sagawa, and Y. Komagata, unpublished observations). It is possible that DCs that loaded mucosal Ags in the gut acquire tolerogenic function and move to systemic lymphoid organs, including the spleen.

We show that the splenic tolerogenic DCs induced by oral Ag play a major role in the active suppression of the experimental murine model of asthma. These findings may provide a new strategy for the management of allergic diseases such as bronchial asthma and for autoimmune diseases. Future studies are needed to investigate how such tolerogenic DCs function in the induction of oral tolerance.

## Acknowledgments

## Disclosures

The authors have no financial conflict of interest.

## References

1. Faria, A. M., and H. L. Weiner. 1999. Oral tolerance: mechanisms and therapeutic applications. Adv. Immunol. 73: 153–264.
2. Weiner, H. L. 2000. Oral tolerance, an active immunologic process mediated by multiple mechanisms. J. Clin. Invest. 106: 935–937.
3. Chen. Y., V. K. Kuchroo, J. Inobe, D. A. Hafler, and H. L. Weiner. 1994. Regulatory T cell clones induced by oral tolerance: suppression of autoimmune encephalomyelitis. Science 265: 1237–1240.
4. Friedman, A., and H. L. Weiner. 1994. Induction of anergy or active suppression following oral tolerance is determined by antigen dosage. Proc. Natl. Acad. Sci. USA 91: 6688–6692.
5. Whitacre, C. C., I. E. Gienapp, C. G. Orosz, and D. M. Bitar. 1991. Oral tolerance in experimental autoimmune encephalomyelitis. III. Evidence for clonal anergy. J. Immunol. 147: 2155–2163.
6. Melamed, D., and A. Friedman. 1993. Direct evidence for anergy in T lymphocytes tolerized by oral administration of ovalbumin. Eur. J. Immunol. 23: 935–942.
7. Melamed, D., and A. Friedman. 1994. In vivo tolerization of Th1 lymphocytes following a single feeding with ovalbumin: anergy in the absence of suppression. Eur. J. Immunol. 24: 1974–1981.
8. Chen, Y., J. Inobe, R. Marks, P. Gonnella, V. K. Kuchroo, and H. L. Weiner. 1995. Peripheral deletion of antigen-reactive T cells in oral tolerance. Nature 376: 177–180.
9. Haneda. K., K. Sano, G. Tamura, T. Sato, S. Habu, and K. Shirato. 1997. TGF-$\beta$ induced by oral tolerance ameliorates experimental tracheal eosinophilia. J. Immunol. 159: 4484–4490.
10. Russo, M., S. Jancar, A. L. Pereira de Siqueira, J. Mengel, E. Gomes, S. M. Ficker, and A. M. Caetano de Faria. 1998. Prevention of lung eosinophilic inflammation by oral tolerance. Immunol. Lett. 61: 15–23.
11. Nakao, A., M. Kasai, K. Kumano, H. Nakajima, K. Kurasawa, and I. Iwamoto. 1998. High-dose oral tolerance prevents antigen-induced eosinophil recruitment into the mouse airways. Int. Immunol. 10: 387–394.
12. Russo, M., M.-A. Nahori, J. Lefort, E. Gomes, A. de Castro Keller, D. Rodriguez, O. G. Ribeiro, S. Adriouch, V. Gallois, A. M. de Faria, and B. B. Vargaftig. 2001. Suppression of asthma-like responses in different mouse strains by oral tolerance. Am. J. Respir. Cell Mol. Biol. 24: 518–526.
13. Zemann, B., C. Schwaerzler, M. Griot-Wenk, M. Nefzger, P. Mayer, H. Schneider, A. de Weck, J. M. Carballido, and E. Lichl. 2003. Oral administration of specific antigens to allergy-prone infant dogs induces IL-10 and TGF-$\beta$ expression and prevents allergy in adult life. J. Allergy Clin. Immunol. 111: 1069–1075.
14. Chung, Y., J. Cho, Y. S. Chang, S. H. Cho, and C. Y. Kang. 2002. Preventive and therapeutic effects of oral tolerance in a murine model of asthma. Immunobiology 206: 408–423.
15. Lider, O., L. M. Santos, C. S. Lee, P. J. Higgins, and H. L. Weiner. 1989. Suppression of experimental autoimmune encephalomyelitis by oral administration of myelin basic protein. II. Suppression of disease and in vitro immune responses is mediated by antigen-specific CD8+ T lymphocytes. J. Immunol. 142: 748–752.
16. Nussenblatt, R. B., R. R. Caspi, R. Mahdi, C. C. Chan, F. Roberge, O. Lider, and H. L. Weiner. 1990. Inhibition of S-antigen induced experimental autoimmune uveoretinitis by oral induction of tolerance with S-antigen. J. Immunol. 144: 1689–1695.
17. Tada, Y., A. Ho, D. R. Koh, and T. W. Mak. 1996. Collagen-induced arthritis in CD4- or CD8-deficient mice: CD8+ T cells play a role in initiation and regulate recovery phase of collagen-induced arthritis. J. Immunol. 156: 4520–4526.
18. Chen, Y., J. Inobe, and H. L. Weiner. 1995. Induction of oral tolerance to myelin basic protein in CD8-depleted mice: both CD4+ and CD8+ cells mediate active suppression. J. Immunol. 155: 910–916.
19. Akbari, O., R. H. DeKruyff, and D. T. Umetsu. 2001. Pulmonary dendritic cells producing IL-10 mediate tolerance induced by respiratory exposure to antigen. Nat. Immunol. 2: 725–731.
20. Dohi, M., S. Tsukamoto, T. Nagahori, K. Shinagawa, K. Saitoh, Y. Tanaka, S. Kobayashi, R. Tanaka, Y. To, and K. Yamamoto. 1999. Noninvasive system for evaluating the allergen-specific airway response in a murine model of asthma. Lab. Invest. 79: 1559–1571.
21. To, Y., M. Dohi, R. Tanaka, A. Sato, K. Nakagome, and K. Yamamoto. 2001. Early interleukin 4-dependent response can induce airway hyperreactivity before development of airway inflammation in a mouse model of asthma. Lab. Invest. 81: 1385–1396.
22. Weiner, H. L. 1997. Oral tolerance: immune mechanisms and treatment of autoimmune diseases. Immunol. Today 18: 335–343.
23. Higuchi, K., M. N. Kweon, K. Fujihashi, J. R. McGhee, and H. Kiyono. 2000. Comparison of nasal and oral tolerance for the prevention of collagen induced murine arthritis. J. Rheumatol. 27: 1038–1044.
24. Hanninen, A., A. Braakhuis, W. R. Heath, and L. C. Harrison. 2001. Mucosal antigen primes diabetogenic cytotoxic T-lymphocytes regardless of dose or delivery route. Diabetes 50: 771–775.
25. Derry, C. J., N. Harper, D. H. Davies, J. J. Murphy, and N. A. Staines. 2001. Importance of dose of type II collagen in suppression of collagen-induced arthritis by nasal tolerance. Arthritis Rheum. 44: 1917–1927.
26. Groux, H., A. O'Garra, M. Bigler, M. Rouleau, S. Antonenko, J. E. de Vries, and M. G. Roncarolo. 1997. A CD4+ T-cell subset inhibits antigen-specific T-cell responses and prevents colitis. Nature 389: 737–742.
27. Gajewski, T. F., and F. W. Fitch. 1988. Anti-proliferative effect of IFN-$\gamma$ in immune regulation. I. IFN-$\gamma$ inhibits the proliferation of Th2 but not Th1 murine helper T lymphocyte clones. J. Immunol. 140: 4245–4252.
28. Fernandez-Botran, R., V. M. Sanders, T. R. Mosmann, and E. S. Vitetta. 1988. Lymphokine-mediated regulation of the proliferative response of clones of T helper 1 and T helper 2 cells. J. Exp. Med. 168: 543–558.
29. Finkelman, F. D., I. M. Katona, T. R. Mosmann, and R. L. Coffman. 1988. IFN-$\gamma$ regulates the isotypes of Ig secreted during in vivo humoral immune responses. J. Immunol. 140: 1022–1027.
30. Belosevic, M., D. S. Finbloom, P. H. Van Der Meide, M. V. Slayter, and C. A. Nacy. 1989. Administration of monoclonal anti-IFN-$\gamma$ antibodies in vivo abrogates natural resistance of C3H/HeN mice to infection with Leishmania major. J. Immunol. 143: 266–274.
31. Scott, P. 1991. IFN-$\gamma$ modulates the early development of Th1 and Th2 responses in a murine model of cutaneous leishmaniasis. J. Immunol. 147: 3149–3155.
32. Webb, D. C., A. N. McKenzie, A. M. Koskinen, M. Yang, J. Mattes, and P. S. Foster. 2000. Integrated signals between IL-13, IL-4, and IL-5 regulate airways hyperreactivity. J. Immunol. 165: 108–113.
33. Hamelmann, E., K. Takeda, A. Haczku, G. Cieslewicz, L. Shultz, Q. Hamid, Z. Xing, J. Gauldie, and E. W. Gelfand. 2000. Interleukin (IL)-5 but not immunoglobulin E reconstitutes airway inflammation and airway hyperresponsiveness in IL-4-deficient mice. Am. J. Respir. Cell Mol. Biol. 23: 327–334.
34. Hamelmann, E., G. Cieslewicz, J. Schwarze, T. Ishizuka, A. Joetham, C. Heusser, and E. W. Gelfand. 1999. Anti-interleukin 5 but not anti-IgE prevents airway inflammation and airway hyperresponsiveness. Am. J. Respir. Crit. Care Med. 160: 934–941.
35. Ying, S., D. S. Robinson, Q. Meng, J. Rottman, R. Kennedy, D. J. Ringler, C. R. Mackay, B. L. Daugherty, M. S. Springer, S. R. Durham, et al. 1997. Enhanced expression of eotaxin and CCR3 mRNA and protein in atopic asthma: association with airway hyperresponsiveness and predominant co-localization of eotaxin mRNA to bronchial epithelial and endothelial cells. Eur. J. Immunol. 27: 3507–3516.
36. Wills-Karp, M., J. Luyimbazi, X. Xu, B. Schofield, T. Y. Neben, C. L. Karp, and D. D. Donaldson. 1998. Interleukin-13: central mediator of allergic asthma. Science 282: 2258–2261.
37. Grünig, G., M. Warnock, A. E. Wakil, R. Venkayya, F. Brombacher, D. M. Rennick, D. Sheppard, M. Mohrs, D. D. Donaldson, R. M. Locksley, and D. B. Corry. 1998. Requirement for IL-13 independently of IL-4 in experimental asthma. Science 282: 2261–2263.
38. Walter, D. M., J. J. McIntire, G. Berry, A. N. McKenzie, D. D. Donaldson, R. H. DeKruyff, and D. T. Umetsu. 2001. Critical role for IL-13 in the development of allergen-induced airway hyperreactivity. J. Immunol. 167: 4668–4675.
39. Wakkach, A., N. Fournier, V. Brun, J. P. Breittmayer, F. Cottrez, and H. Groux. 2003. Characterization of dendritic cells that induce tolerance and T regulatory 1 cell differentiation in vivo. Immunity 18: 605–617.
40. Sato, K., N. Yamashita, N. Yamashita, M. Baba, and T. Matsuyama. 2003. Regulatory dendritic cells protect mice from murine acute graft-versus-host disease and leukemia relapse. Immunity 18: 367–379.
41. Legge, K. L., R. K. Gregg, R. Maldonado-Lopez, L. Li, J. C. Caprio, M. Moser, and H. Zaghouani. 2002. On the role of dendritic cells in peripheral T cell tolerance and modulation of autoimmunity. J. Exp. Med. 196: 217–227.
42. Alpan, O., G. Rudomen, and P. Matzinger. 2001. The role of dendritic cells, B cells, and M cells in gut-oriented immune responses. J. Immunol. 166: 4843–4852.
43. Akbari, O., G. J. Freeman, E. H. Meyer, E. A. Greenfield, T. T. Chang, A. H. Sharpe, G. Berry, R. H. DeKruyff, and D. T. Umetsu. 2002. Antigen-specific regulatory T cells develop via the ICOS-ICOS-ligand pathway and inhibit allergen-induced airway hyperreactivity. Nat. Med. 8: 1024–1032.
44. Alpan, O., E. Bachelder, E. Isil, H. Arnheiter, and P. Matzinger. 2004. "Educated" dendritic cells act as messengers from memory to naïve T helper cells. Nat. Immunol. 5: 615–622.
45. Shortman, K., and Y. J. Liu. 2002. Mouse and human dendritic cell subtypes. Nat. Rev. Immunol. 2: 151–161.

# A functional variant in *FCRL3*, encoding Fc receptor-like 3, is associated with rheumatoid arthritis and several autoimmunities

Yuta Kochi[1,2], Ryo Yamada[1], Akari Suzuki[1], John B Harley[3], Senji Shirasawa[4], Tetsuji Sawada[2], Sang-Cheol Bae[5], Shinya Tokuhiro[1], Xiaotian Chang[1], Akihiro Sekine[6], Atsushi Takahashi[7], Tatsuhiko Tsunoda[7], Yozo Ohnishi[8], Kenneth M Kaufman[3], Changsoo Paul Kang[9], Changwon Kang[9], Shigeru Otsubo[10], Wako Yumura[11], Akio Mimori[4], Takao Koike[12], Yusuke Nakamura[10,13], Takehiko Sasazuki[4] & Kazuhiko Yamamoto[1,2]

Rheumatoid arthritis is a common autoimmune disease with a complex genetic etiology. Here we identify a SNP in the promoter region of *FCRL3*, a member of the Fc receptor-like family, that is associated with susceptibility to rheumatoid arthritis (odds ratio = 2.15, *P* = 0.00000085). This polymorphism alters the binding affinity of nuclear factor-κB and regulates *FCRL3* expression. We observed high *FCRL3* expression on B cells and augmented autoantibody production in individuals with the disease-susceptible genotype. We also found associations between the SNP and susceptibility to autoimmune thyroid disease and systemic lupus erythematosus. *FCRL3* may therefore have a pivotal role in autoimmunity.

Rheumatoid arthritis is one of the most common autoimmune diseases and is characterized by inflammation of synovial tissue and joint destruction. Although the disease is believed to result from a combination of genetic and environmental factors, its complete etiology has not yet been clarified[1]. Specific haplotypes of human leukocyte antigen (HLA)-DRB1, usually referred to as shared-epitope sequences[2], have been repeatedly reported to confer susceptibility to rheumatoid arthritis[3,4]; other genetic components are also involved[5]. This combination of HLA haplotypes and non-HLA genes accounting for disease susceptibility is also observed for other autoimmune diseases[6–8]. In autoimmune thyroid disease (AITD), for instance, the HLA-DR3 haplotype is associated with disease risk, as is a functional haplotype of a non-HLA gene, *CTLA4*, that has recently been associated with AITD susceptibility[9].

Identification of non-HLA genes associated with rheumatoid arthritis susceptibility and other autoimmunities seems difficult, because of the low relative risk of disease resulting from these non-HLA genes compared with the strong relative risk from disease-associated HLA haplotypes. In a search for non-HLA determinants

of disease susceptibility, whole-genome studies have been done for both human autoimmune diseases and experimental animal models. These studies have identified nonrandom clustering of susceptibility loci for clinically distinct diseases[8,10]. The overlap of susceptibility loci for multiple autoimmunities suggests that common susceptibility genes exist in those regions. Intense studies of loci-clustering regions identified genes commonly associated with multiple autoimmune diseases, such as *CTLA4* on 2q33 (ref. 9), *SLC22A4* and *SLC22A5* on 5q31 (ref. 11) and *PTPN22* on 1p13 (ref. 12).

Cytoband 1q21–23 is one of the regions implicated in susceptibility to multiple autoimmune diseases. The Fcγ receptor (FcγR) II/III genes are located at 1q23, and a new family of genes, Fc receptor-like genes (FCRLs, also known as FcRHs[13,14], IRTAs[15,16] or SPAPs[17]), clusters nearby at 1q21 (**Fig. 1a**). FCRLs have high structural homology with classical FcγRs, although their ligands and function are not yet known. These receptors are good candidates for involvement in autoimmunity, as they are believed to be involved in the pathogenesis of rheumatoid arthritis and other autoimmune diseases[18]. Region 1q23 is a candidate locus for susceptibility to systemic lupus erythematosus
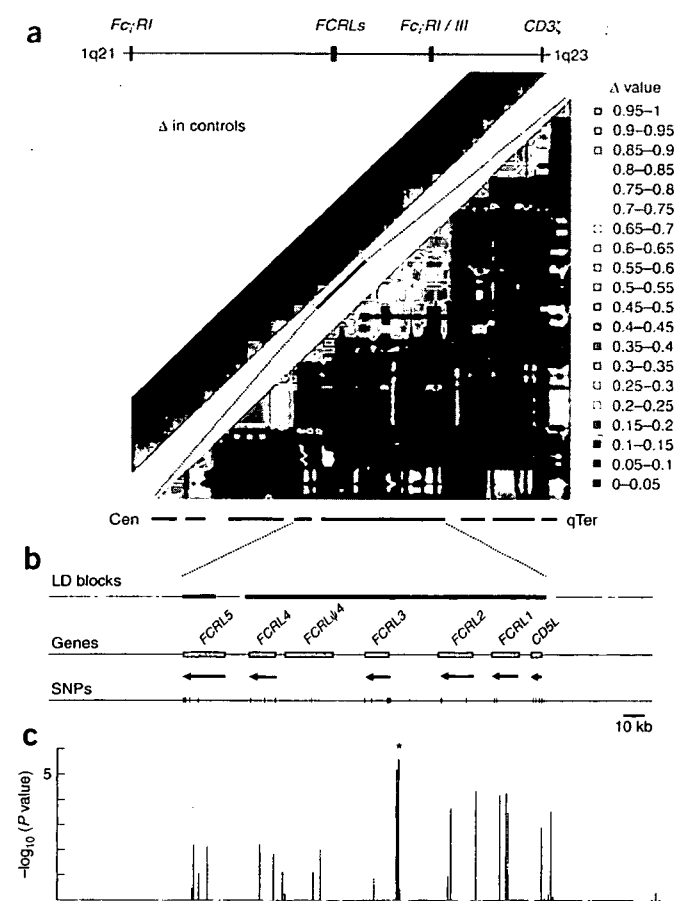
**Figure 1** LD and association of the FCRL gene cluster. (a) Pairwise LD between SNPs, as measured by Δ in 658 controls. The 16-Mb region in 1q21–23 (upper left) and the 2-Mb region around the FCRL gene cluster (lower right) were evaluated. (b) Location of LD blocks, genes and 41 SNPs in the FCRL gene cluster. (c) Case-control association test with 41 SNPs in the FCRL gene cluster using 830 affected individuals and 658 controls. *Peak association.

rheumatoid arthritis–susceptibility genes, the association of classical FcγRs with disease susceptibility remains controversial[26,27]. Here we focused on the 1q21–23 region to identify rheumatoid arthritis–associated genes in Japanese subjects using linkage disequilibrium (LD) mapping.

## RESULTS
### Case-control study by SNP-based LD mapping at 1q21–23

To evaluate the extent of association, we analyzed LD with SNPs distributed in a 16-Mb region on 1q21–23, including the FCRL gene cluster and the classical FcγRs (**Fig. 1a**). We genotyped 658 control subjects for 742 SNPs from the JSNP database and selected 491 SNPs with allele frequency $>0.1$, successful genotyping rate $>0.95$ and $P > 0.01$ with Hardy-Weinberg equilibrium testing for evaluation of LD. We calculated the pairwise LD index Δ (ref. 28) for each pair of SNPs, identifying 110 LD blocks[11] at a threshold of $\Delta > 0.5$ (**Fig. 1a**).

For association testing, we examined the Japanese set of 830 cases and 658 controls used for LD block evaluation. We initially genotyped 94 rheumatoid arthritis cases for 491 SNPs and compared their allele frequencies with those of 658 control subjects. We identified nine SNPs that had allele frequencies differing by more than 0.1 between 658 controls and 94 cases with $P < 0.01$. We genotyped the remaining cases for these nine SNPs and tested their allele frequencies for case-control association. We identified the smallest $P$ value between an intronic SNP in the gene FCRL3 and rheumatoid arthritis (fcrl3_6, $P = 1.8 \times 10^{-5}$; association was statistically significant in both rheumatoid arthritis subgroups (94 and 736 individuals)). This SNP was located in a LD block containing four of the five FCRL genes; the fifth was in the adjacent block. We therefore evaluated the origin of this association in these two LD blocks (**Fig. 1b**), although our results do not exclude the presence of variants associated with rheumatoid arthritis or other autoimmune diseases in other LD blocks at 1q21–23.

In addition to the 25 SNPs of the 491 that we used for LD block evaluation, we identified 16 additional SNPs in exons and 5′ and 3′ flanking regions of five FCRL genes and one pseudogene (FCRLψ4) by searching the public database and sequencing genomic DNA from Japanese individuals with rheumatoid arthritis. We genotyped these 16 SNPs in the identical case and control samples (830 cases, 658 controls) to increase the density of variants in the targeted region. We observed a peak of association in a short segment consisting of four SNPs in FCRL3 ($P < 1.0 \times 10^{-4}$; **Fig. 1c** and **Supplementary Table 1** online): fcrl3_3, fcrl3_4, fcrl3_5 and fcrl3_6, located at nt −169, −110, +358 (5′ untranslated region of exon 2) and +1381 (intron 3; 204 bp and 859 bp from the 3′ and 5′ ends of the flanking exons) relative to the transcription initiation site, respectively.

We observed the smallest $P$ value without correction in recessive-trait genotype comparison of fcrl3_3 in FCRL3 ($P = 8.5 \times 10^{-7}$; odds ratio = 2.15; 95% confidence interval = 1.58–2.93; **Table 1**). This

(SLE), and variants in the classical FcγR II/III genes partially account for disease susceptibility[6,19]. Region 1q21 is a candidate locus for susceptibility to psoriasis (PSORS4; refs. 7,20) and multiple sclerosis[21]. The mouse homologous region to human 1q21, on chromosome 3, also contains susceptibility loci for multiple autoimmune disease models[8], including collagen-induced arthritis (Cia5, also called Mcia2 (ref. 22); Eae3 (ref. 23); Tmevd2 (ref. 24); Idd10; and Idd17 (ref. 25)). Although 1q21–23 is a good candidate region for containing

**Table 1 Case-control analysis of FCRL3**

| SNP | Location | Allele (1/2) | Allele 1 frequency | | Genotype 11 versus 12 + 22 | | |
| | | | Affected individuals | Controls | OR (95% c.i.) | $\chi^2$ | P |
| --- | --- | --- | --- | --- | --- | --- | --- |
| fcrl3_3 | −169 | C/T | 0.42 | 0.35 | 2.15 (1.58–2.93) | 24.3 | 0.00000085 |
| fcrl3_4 | −110 | A/G | 0.25 | 0.18 | 3.01 (1.71–5.29) | 16.1 | 0.000060 |
| fcrl3_5 | Exon 2 | C/G | 0.42 | 0.35 | 2.05 (1.51–2.78) | 21.6 | 0.0000033 |
| fcrl3_6 | Intron 3 | A/G | 0.42 | 0.34 | 2.02 (1.49–2.75) | 20.8 | 0.0000052 |

SNPs with $P < 0.0001$ in allele frequency comparison test are shown. c.i., confidence interval; OR, odds ratio.

— 162 —

### Table 2 Haplotype structure and frequency in *FCRL3*

| Haplotype | Sequence (fcrl3_3-4-5-6) | Frequency | |
|---|---|---|---|
| | | Affected individuals | Controls |
| 1 | TGGG | 0.58 | 0.65 |
| 2 | CACA | 0.25 | 0.19 |
| 3 | CGCA | 0.17 | 0.14 |

Haplotypes with frequency >0.01 are shown.

*P* value was still significant when the most conservative Bonferroni correction was applied (comparisons for 507 SNPs; corrected *P* = 0.00043). The four strongly associated SNPs were in LD with each other, and we inferred three common haplotypes (**Table 2**); fcrl3_3, fcrl3_5 and fcrl3_6 showed strong LD with each other ($\Delta > 0.99$), whereas fcrl3_4 showed relatively weak LD with the other three SNPs (mean $\Delta = 0.68$).

To identify causal variants in this segment on the basis of genotype data, we carried out a forward stepwise-regression procedure with a cut-off *P* value to proceed to the next step of 0.01 (ref. 29). No SNP in FCRL genes other than *FCRL3* improved the model. None of the four SNPs in *FCRL3* were preferred over the others in these data (data not shown). This result implied that one of the SNPs in *FCRL3* might cause the disease, but the possibility remained that variants in other genes were truly associated with the disease.

To validate the case-control association test, we evaluated the impact of population stratification on the case-control study (830 cases, 658 controls). We selected 2,069 SNPs, each of which was identified as a tagging SNP[30] in 2,069 distinct LD segments that were previously identified by genotyping 74,842 SNPs distributed in

autosomal chromosomes[31]. We analyzed population structure[32] and the $\chi^2$ sum[33] to evaluate stratification but detected no significant evidence of population stratification (**Supplementary Fig. 1** online). These results are suggestive of no or negligible stratification of our samples and support the validity of the case-control association results by removing this confounding factor from further consideration.

### Regulatory effect of SNP $-169C \rightarrow T$ on *FCRL3* expression

Because none of the four SNPs in *FCRL3* (fcrl3_3, fcrl3_4, fcrl3_5 and fcrl3_6) produces amino-acid substitutions, we assessed potential effects of the SNPs on transcription factor binding using TRANSFAC software. Nuclear factor-κB (NF-κB) was predicted to bind the sequence containing the rheumatoid arthritis–susceptibility allele fcrl3_3 ($-169C$) with a high score (core match 1.000, matrix match 0.957); substitution with the nonsusceptible allele T decreased the score of NF-κB binding substantially (core match 0.760, matrix match 0.824). The other three SNPs were not predicted to bind to any transcriptional factor with high score, and nucleotide substitution was not predicted to affect binding at any regulatory factor. We therefore focused on the 5′ flanking region of fcrl3_3 to explore the regulatory effects on expression of *FCRL3*.

We carried out reporter gene analysis using the genomic sequence of *FCRL3* from nt $-523$ to $+203$. We made constructs corresponding to the three haplotypes using SNPs at nt $-169$ ($C \rightarrow T$, fcrl3_3) and $-110$ ($G \rightarrow A$, fcrl3_4; **Fig. 2a**) and used them to transfect Raji cells, a Burkitt's lymphoma cell line that expresses *FCRL3* (ref. 13) and is derived from germinal center B cells. Luciferase activity was substantially greater in cells transfected with $-169C -110G$ or $-169C -110A$ constructs than in cells transfected with $-169T -110G$ constructs. This suggests that SNP $-169C \rightarrow T$ is crucial for regulation of *FCRL3* expression. To clarify, we cloned single or four tandem copies of 30-bp
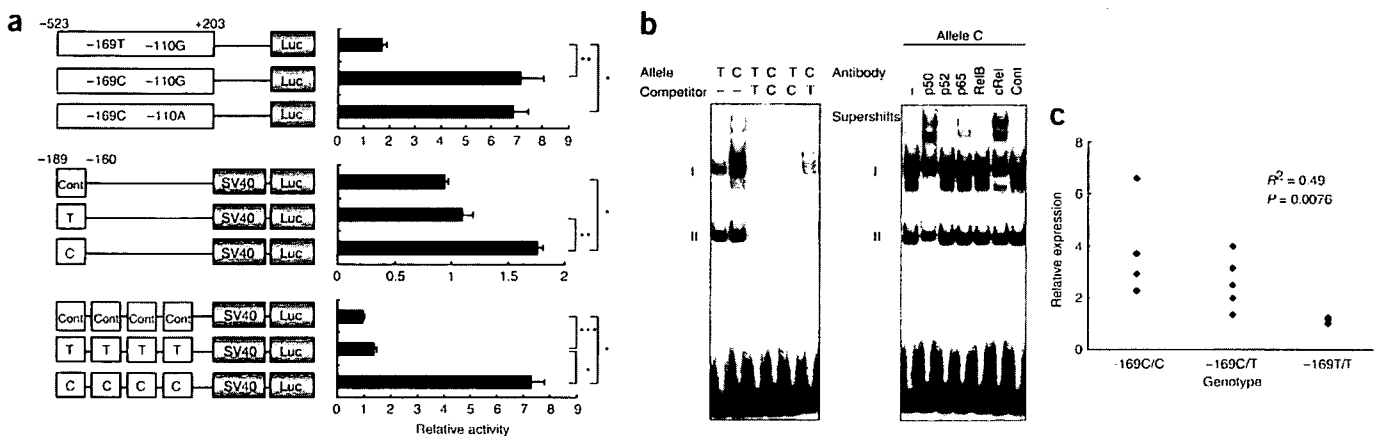


**Figure 2** Correlation of *FCRL3* expression with allele and genotype. (a) Promoter activity of haplotypes in *FCRL3* (top) and enhancing activity of the 30-bp promoter region around $-169C \rightarrow T$ (middle and bottom), as evaluated by luciferase assay. Data represent mean ± s.e.m. Representative data from three experiments done in quadruplicate. $*P < 0.0001$; $**P < 0.001$; $***P < 0.01$ by Student's *t*-test. (b) Binding affinity of nuclear factors to the 30-bp promoter region around $-169C \rightarrow T$ evaluated by EMSA. Allelic difference and competition experiment (left) and supershift experiment using antibodies for NF-κB components (right). (c) Expression of *FCRL3* measured by quantitative TaqMan PCR of RNA purified from CD19⁺ B cells obtained from 13 healthy volunteers (C/C, *n* = 4; C/T, *n* = 5; T/T, *n* = 4). (d) ASTQ. *FCRL3* transcripts in B cells and genomic DNA from individuals (*n* = 5) with heterozygous genotypes ($-169$C/T $+358$C/G) were amplified and quantified using an *Eag*I restriction-fragment length polymorphism located at position $+358$. The 122-bp and 85-bp bands represent transcripts of the $+358$C allele and $+358$G allele, respectively. Transcripts from homozygous individuals ($+358$C/C and $+358$G/G) are shown as controls for digestion.
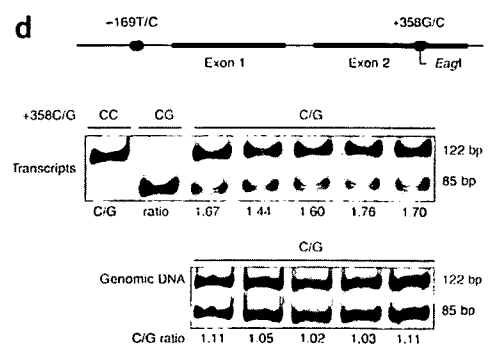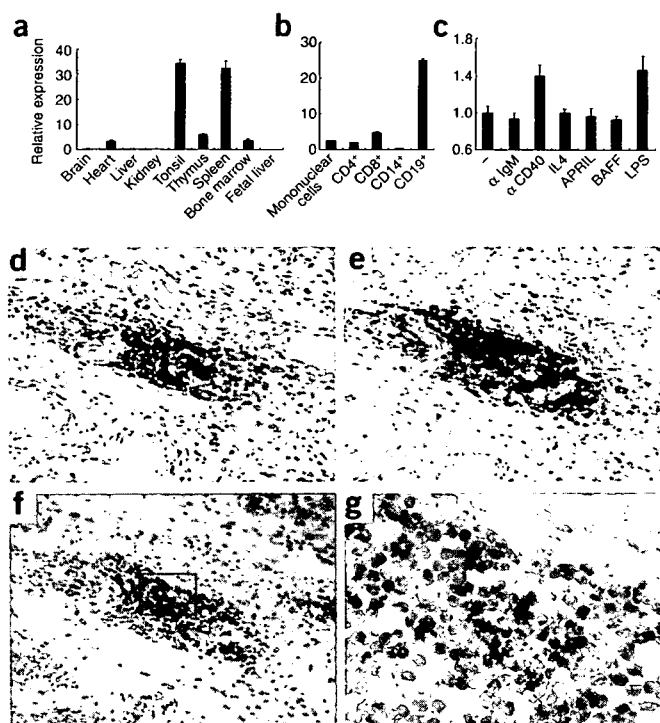
**Figure 3** Expression patterns of *FCRL3* in human tissues and cells.
(a) Relative expression of *FCRL3* in various tissues. (b) Relative expression of *FCRL3* in fractionated leukocytes using MTC panel (Clontech).
(c) Relative expression of *FCRL3* in response to stimuli (antibody to CD40, 1 µg ml$^{-1}$; antibody to IgM, 1 µg ml$^{-1}$; IL-4, 10 ng ml$^{-1}$; APRIL, 10 ng ml$^{-1}$; BAFF, 10 ng ml$^{-1}$; LPS, 100 ng ml$^{-1}$) for 4 h. Representative data from three experiments done in triplicate. (d,e) Lymphocyte aggregates in rheumatoid arthritis synovium. T cells and B cells in serial sections were immunostained using antibodies to CD3 (d) and CD20 (e), respectively. (f,g) *FCRL3* mRNA expression (blue stain) in rheumatoid arthritis synovium as analyzed by *in situ* hybridization. Higher magnification views of synovium (g) are denoted by the box in f (magnifications: d–f, ×100; g, ×400). Counterstaining: d,e, hematoxylin; f,g, nuclear fast red.

oligonucleotides surrounding SNP −169C→T and control oligonucleotides into a vector with the SV40 promoter. Cells transfected with a single copy of the C allele produced substantially greater luciferase activity than cells transfected with a single copy of the T allele. More convincingly, transfection with four tandem copies of the C allele enhanced luciferase activity by a factor of 20 over transfection with four tandem copies of the T allele (**Fig. 2a**).

To elucidate specific nuclear factors that bind the disease-susceptible allele, we analyzed the sequence around −169C→T. These sequences were predicted by TRANSFAC software to have binding affinity for NF-κB, which regulates a wide variety of genes in the immune system. The disease-susceptible sequence (including −169C) had higher matrix similarity to the consensus NF-κB binding motif than the nonsusceptible sequence (including −169T). We then carried out electrophoretic mobility shift assays (EMSAs) to examine whether differences between the susceptible −169C allele and the nonsusceptible −169T allele affected binding of nuclear proteins from Raji cells. We used the same 30-bp labeled oligonucleotides used in the luciferase assay. These sequences contain the predicted NF-κB binding site. We observed two main bands, I and II, in the presence of nuclear extracts; the intensity of band I was higher for the susceptible −169C allele than for the nonsusceptible −169T allele (**Fig. 2b**). Competition assays with

unlabeled oligonucleotides indicated that these complexes were specific for the probes. In addition, competition assays with unlabeled probes of the C allele for T and the T allele for C showed that the C allele was better able to compete for binding, a result consistent with the higher binding affinity of labeled C allele probes alone. We also carried out a supershift experiment with antibodies specific for NF-κB components (p50, p52, p65, RelB and cRel). We observed supershifts in some lanes with specific antibodies for p50, p65 and cRel (**Fig. 2b**). Among these, only antibody to p50 shifted band II, suggestive of the presence of a p50-p50 homodimer. Band I had the highest intensity and a substantial allelic difference and was supershifted by antibodies to p50, p65 and cRel. Although these findings indicate that band I comprises a mixture of heterodimers, the greater shifts caused by antibodies to p50 and cRel suggest that the main component is a p50-cRel heterodimer.

The two *in vitro* assays showed the potent transcriptional activity of the disease-susceptible haplotype regulated by NF-κB, suggesting that expression of *FCRL3* is greater from the disease-susceptible −169C allele than from the nonsusceptible −169T allele. To extend these findings, we quantified expression of *FCRL3* in peripheral blood B cells from healthy donors using quantitative TaqMan methods and analyzed the effect of the number of susceptible copies on the transcript level by regression model. Regression analysis identified a significant positive correlation between number of susceptible chromosomes and transcription level ($R^2 = 0.49$, $P = 0.0076$; **Fig. 2c**).

We also carried out allele-specific transcript quantification[9,34] to confirm the effect of the SNP on transcription. Using an *Eag*I restriction-fragment length polymorphism located at position +358 in exon 2 of *FCRL3* (fcrl3_5, +358C→G), we measured the relative contribution of each haplotype to transcript production in heterozygous individuals (**Fig. 2d**). We evaluated the transcripts of five doubly heterozygous individuals with genotype −169C/T +358C/G; the mean ratio (susceptible versus nonsusceptible haplotype) was 1.63, significantly higher than that of DNA amplicons (ratio = 1.06, $P < 1 \times 10^{-5}$) from the same individuals. (The quantity of template DNA from the two haplotypes was equal.) These results show that the

**Table 3 Genotype and autoantibodies in individuals with rheumatoid arthritis**

| Genotype | RF | | Antibody to CCP | |
| --- | --- | --- | --- | --- |
| | $n^a$ | Serum level$^b$ (IU/ml) | $n^c$ | Positivity (%) |
| −169C/C | 29 | 479.9 ± 91.3$^d$ | 17 | 100.0$^e$ |
| −169C/T | 75 | 323.7 ± 47.3$^d$ | 35 | 94.3$^e$ |
| −169T/T | 44 | 216.4 ± 44.0$^d$ | 19 | 73.7$^e$ |

$^a$N = 148. $^b$Mean ± s.e.m. $^c$N = 71. $^dR^2$ = 0.049, P = 0.0065 by regression analysis. $^eP$ = 0.029 by Fisher's exact test.

# ARTICLES

Table 4 Association of SNP −169C→T with AITD and SLE

| Disease | n | Genotype | | | Allele C frequency | Recessive-trait comparison | | |
| | | CC | CT | TT | | OR (95% c.i.) | $\chi^2$ | P |
| --- | --- | --- | --- | --- | --- | --- | --- | --- |
| GD | 351 | 72 | 179 | 100 | 0.46 | 1.79 (1.34–2.39) | 15.7 | 0.000074 |
| HT | 158 | 30 | 74 | 54 | 0.42 | 1.62 (1.07–2.47) | 5.2 | 0.022 |
| AITD total | 509 | 102 | 253 | 154 | 0.45 | 1.74 (1.35–2.24) | 18.5 | 0.000017 |
| SLE | 564 | 100 | 259 | 205 | 0.41 | 1.49 (1.16–1.92) | 9.8 | 0.0017 |
| RA* + AITD + SLE | 2,437 | 438 | 1,167 | 832 | 0.42 | 1.52 (1.29–1.79) | 24.2 | 0.00000084 |
| Control | 2,037 | 257 | 995 | 785 | 0.37 | | | |

*Rheumatoid arthritis represents sum of three sets (n = 1,364). c.i., confidence interval; GD, Graves' disease; HT, Hashimoto's thyroiditis; OR, odds ratio; RA, rheumatoid arthritis.

expression of FCRL3 is higher in individuals with the disease-susceptible haplotype and suggest that higher expression of FCRL3 is a potential cause and component of the pathological mechanism(s) leading to rheumatoid arthritis.

## Expression of FCRL3 mRNA

We then quantified FCRL3 expression in multiple tissues using Taq-Man methods. Expression of FCRL3 transcripts was high in the spleen and tonsils (Fig. 3a), which are secondary lymphoid organs. We observed lower expression in thymus and bone marrow. In human blood fractions, CD19+ cells, which represent the B-cell population, had the greatest FCRL3 expression among peripheral blood mononuclear cells. CD4+ and CD8+ cells had less expression (Fig. 3b). We next examined the effect of B-cell stimulation on FCRL3 expression. We cultured peripheral blood B cells from a healthy donor for 4 h using known B-cell stimulants and then quantified FCRL3 mRNA (Fig. 3c). Expression of FCRL3 was increased by antibody to CD40 and lipopolysaccharide (LPS).

We then investigated expression of FCRL3 transcripts in synovial tissue using in situ hybridization methods. T and B cells are the key players with regard to inflammation in synovial tissue, producing proinflammatory cytokines and autoantibodies that might be pathogenic[1]. These cells show three distinct histological patterns: diffuse infiltration, clustering in aggregates and follicles with germinal-center reaction[35,36]. We observed aggregations of T and B cells in paraffin-embedded synovial sections from individuals with rheumatoid arthritis, using immunostaining with antibodies to CD3 and CD20, respectively (Fig. 3d,e). In situ hybridization assay with serial sections detected FCRL3 mRNA in aggregated lymphocytes (Fig. 3f,g). Although strict differentiation between B and T cells was difficult, at least some aggregated B cells were positive, with strong expression of FCRL3 mRNA. Synovium from two other individuals with rheumatoid arthritis had similar lymphocyte aggregates and FCRL3 expression (Supplementary Fig. 2 online).

## SNP association with autoantibody and HLA-DRB1 status

Because we suspected that higher FCRL3 expression led to B-cell abnormalities in rheumatoid arthritis, we examined associations in individuals with rheumatoid arthritis between genotype and two rheumatoid arthritis–related autoantibodies: rheumatoid factor (RF) and antibody to cyclic citrullinated peptide (CCP). RF is a well-known autoantibody for the Fc region of IgG, and titers correlate with rheumatoid arthritis disease activity[37]. Antibody to CCP recognizes peptides containing citrulline and is detected in rheumatoid arthritis with extremely high specificity[38,39]. RF titer in individuals with rheumatoid arthritis was significantly positively correlated with the number of susceptible alleles ($R^2$ = 0.049, P = 0.0065; Table 3). The

positive ratio of antibody to CCP in individuals with rheumatoid arthritis also differed significantly among genotypes (P < 0.05) and correlated with number of susceptible alleles.

Because genetic interactions between HLA and non-HLA loci have been described in susceptibility for rheumatoid arthritis and other autoimmune diseases[26,40], we compared genotype distributions for SNP −169C→T among three rheumatoid arthritis subgroups stratified by number of HLA-DRB1 shared-epitope alleles. We previously genotyped HLA-DRB1 in our population and observed significant associations between rheumatoid arthritis susceptibility and shared-epitope alleles[4]. Allele frequency of the rheumatoid arthritis–susceptibility allele −169C was significantly higher in the subgroup with two copies of shared-epitope alleles (0.49, n = 113) than in the subgroup with no shared-epitope alleles (0.39, n = 215; P < 0.05).

## Replication study of association in three autoimmunities

To confirm associations between the FCRL3 variant and rheumatoid arthritis susceptibility, we carried out a replication study (540 individuals with rheumatoid arthritis, 636 controls). We compared allele frequency and found a significant association between fcrl3_3 (−169C→T) and rheumatoid arthritis susceptibility (allele frequency was 0.40 in individuals with rheumatoid arthritis versus 0.46 in controls; P = 0.041; Supplementary Table 2 online). We noted no significant differences between two cohorts that consisted of the replication samples. These results further confirmed the association of the fcrl3_3 −169C allele with rheumatoid arthritis susceptibility in Japanese individuals.

Because this region is associated with multiple autoimmune diseases, and because several variants are involved in multiple autoimmunities, we investigated associations between SNP −169C→T and two other autoimmune diseases: AITD and SLE. We recruited 509 Japanese individuals with AITD (351 with Graves' disease and 158 with Hashimoto's thyroiditis) and 564 Japanese individuals with SLE and compared them with 2,037 Japanese controls. In addition, we combined AITD, SLE and rheumatoid arthritis cases as subjects with an autoimmune phenotype and tested for associations with the SNP. Individual diseases, as well as combination of two AITDs and combination of AITD, SLE and rheumatoid arthritis, were significantly associated with the SNP (odds ratio = 1.52, P = 0.00000084 in Japanese for a recessive model between all four autoimmunities considered in aggregate and controls; Table 4). As rheumatoid arthritis–specific autoantibodies were correlated with the number of susceptible alleles, antibody to DNA titer was higher in individuals with SLE with genotype −169C/C than in subjects with other genotypes (294.1 IU ml$^{-1}$ versus 145.5 IU ml$^{-1}$; n = 120; P = 0.026 by Student's t-test), a conclusion not further established by regression analysis (P = 0.12).

## DISCUSSION

LD mapping of 1q21–23 in Japanese subjects identified multiple LD blocks in the region, and one block containing FCRL3 was associated with rheumatoid arthritis. This association was replicated in a second Japanese case-control set. The rheumatoid arthritis–associated allele was also associated with increased risk of other autoimmune disorders, such as AITD (Graves' disease and Hashimoto's thyroiditis) and SLE. Recent reports on autoimmune disease–associated polymorphisms show that some disease-susceptible variants are limited to specific ethnic groups[12] whereas others are widely dispersed but significantly associated with disease in only specific ethnic groups[41,42]. We evaluated four-SNP haplotypes in FCRL3 in African American, European American and Asian (Korean and Japanese) subjects and found weaker LD in African Americans than in other groups and substantial differences in allelic frequency among the groups (Supplementary Table 3 online).

Although the evidence presented here for FCRL3 being an auto-immune disease–susceptibility gene is powerful, additional autoimmune disease–related genes probably exist in this region. For example, 1q23 is a good candidate locus for SLE susceptibility[6], particularly involving the association of the classical FcγR genes with SLE susceptibility in the Japanese population[19], although those variants are not in LD with SNP −169C→T in our Japanese subjects ($\Delta < 0.05$, Fig. 1a). Multiple SLE susceptibility genes are also homologous to human 1q23 in mouse models of SLE[43].

Further evaluation of polymorphism associations showed that a SNP in the promoter region of FCRL3 alters expression of FCRL3 through NF-κB binding. Because higher expression of FCRL3 was observed in individuals with susceptible alleles, and augmented auto-antibody production was associated with the susceptible genotype, important steps in the sequence of events leading to autoimmunity must proceed through FCRL3. That the susceptible allele is associated with HLA-DRB1 in rheumatoid arthritis is consistent with FCRL3 functioning in the context of HLA class II restriction, which is usually seen in the interaction between T cells and antigen-presenting cells, including B cells. Moreover, together with the dominant expression of FCRL3 on B cells and the importance of B cells suggested by a recent clinical trial of B cell–depleting therapy[44], the present findings might provide a genetic basis for B-cell abnormality in autoimmunity.

Although the precise function of FCRL3 is unknown, its predicted molecular structure suggests that it is a membranous protein that conveys signals into cells through a cytoplasmic domain containing an immunoreceptor-tyrosine activation motif and an immunoreceptor-tyrosine inhibitory motif[14]. An in vitro study showing the binding of tyrosine kinases syk and ZAP70 to the immunoreceptor-tyrosine activation motif region and of tyrosine phosphatases SHP-1 and SHP-2 to the immunoreceptor-tyrosine inhibitory motif region[17] supports the proposed signaling function of FCRL3. In a previous study examining in situ hybridization in human tonsil, FCRL3 was expressed in the germinal center, with particularly high expression in the light zone[16], suggesting that FCRL3 functions predominantly in centrocytes. The present finding that CD40 stimulation, which is important in germinal-center formation[45], upregulates FCRL3 expression in B cells could indicate that FCRL3 is specifically expressed in germinal-center centrocytes under the influence of CD40 signals. In the light zone, centrocytes undergo clonal selection and affinity maturation regulated by positive and negative signals from antigen receptors and coreceptors[46]. High expression of FCRL3 and augmented autoantibody production in individuals with the disease-susceptible genotype is consistent with the idea that FCRL3 influences the fate of B cells and augments the emergence of self-reactive cells in the germinal center.

In addition to its role in lymphoid tissues, expression of FCRL3 in synovial tissue might explain the pathological connection between FCRL3 variants and rheumatoid arthritis. FCRL3 is strongly expressed in aggregated lymphocytes. Although our synovial samples showed only T-cell–B-cell aggregates, lymphocytes in rheumatoid arthritis synovial tissue are known to form a germinal center–like structure, called an ectopic germinal center, where T cell–dependent antibody production and affinity maturation occur[36]. Ectopic germinal-center formation also occurs in tissues from individuals with AITD and SLE, and FCRL3 might be involved in pathological autoimmune reaction in these disease-specific ectopic lymphocyte aggregates.

Considering that augmented expression of FCRL3 is associated with susceptibility to autoimmune disorders, and that FCRL3 expression is regulated in B cells in the secondary lymphoid organ and is detected in lymphocytes of disease-specific tissues, FCRL3 probably functions in immunity and potentially pathogenic in autoimmune disorders.

## METHODS

**Subjects.** We enrolled three independent cohorts of individuals with rheumatoid arthritis ($n = 830$, 217 and 323), a cohort of individuals with SLE ($n = 564$) and a cohort of individuals with AITD ($n = 509$) comprising Graves' disease ($n = 351$) and Hashimoto's thyroiditis ($n = 158$) through several medical institutes in Japan. We recruited four independent cohorts of unaffected control subjects ($n = 658$, 262, 374 and 752) at various sites in Japan. All subjects were Japanese. Individuals with rheumatoid arthritis (84.2% women; age $59.0 \pm 12.3$ years (mean ± s.d.); 75.0% RF-positive) satisfied the revised criteria of the American Rheumatism Association for rheumatoid arthritis[47]. Individuals with SLE satisfied the criteria of the American College of Rheumatology for SLE[48]. Diagnosis of AITD was established on the basis of clinical findings and results of routine examinations for circulating thyroid hormone and thyroid-stimulating hormone concentrations, serum levels of antibodies against thyroglobulin, thyroid microsomes and thyroid-stimulating hormone receptors, ultrasonography, $^{99m}$TCO$_4^-$ (or $[^{123}$I]) uptake and thyroid scintigraphy.

We evaluated LD at 1q21–23 in the first control cohort compared with the first rheumatoid arthritis cohort to identify the rheumatoid arthritis–associated LD block and SNPs. The second and third rheumatoid arthritis and control cohorts were used for replication testing of results from the first cohorts. We tested Graves' disease; Hashimoto's thyroiditis; SLE; the combination of the two AITDs; and the combination of rheumatoid arthritis, SLE and the two AITDs for associations using the total pool of controls. We enrolled control subjects from three other ethnic groups, Korean ($n = 100$), African American ($n = 120$) and European American ($n = 120$), for evaluation of FCRL3 haplotypes. We sampled synovial tissues from individuals with rheumatoid arthritis who underwent arthroplastic surgery. All subjects provided informed consent to participate in the study, as approved by the ethical committee of the SNP Research Center, RIKEN.

**SNPs and genotyping.** We identified SNPs in exons and 5′ and 3′ flanking regions of FCRL1, FCRL2, FCRL3 and FCRLψ4 by direct sequencing of DNA from 24 individuals. We selected other SNPs from the JSNP and Assay-On-Demand SNP databases (Applied Biosystems). We genotyped SNPs using Invader and TaqMan assays[41] as indicated by the manufacturers. Probe sets for the Invader assay were designed and synthesized by Third Wave Technologies, and those for the TaqMan assay were obtained from Applied Biosystems. When assessing the results of SNP genotyping, we generally excluded successful call rates <0.95 and values of $P < 0.01$ obtained by Hardy-Weinberg equilibrium testing in control subjects. The error rate of Invader assay was 0.0023, which was estimated by 11,092 assays in two replicates using 118 randomly selected SNPs (internal control data).

**Luciferase assay.** We cloned the promoter fragment of three haplotypes corresponding to nt −523 to +203 of FCRL3 into the pGL3-Basic vector (Promega). We generated oligonucleotides using the allelic sequences of nt −189 to −160 of FCRL3. We cloned a single copy or four tandem copies of

— 166 —

# ARTICLES

these oligonucleotides into pGL3-Promoter vector (Promega). We grew Raji cells (RCB1647; RIKEN Cell Bank) in RPMI1640 medium supplemented with 10% fetal bovine serum and antibiotics. We electroporated (230 V and 975 μF) $1 \times 10^7$ cells with 5 pmol of constructs and 1 pmol of pRL-TK vector (internal control for transfection efficiency) in a 0.4-cm gap cuvette. After 48 h, we collected cells and measured luciferase activity using the Dual-Luciferase Reporter Assay System (Promega).

**EMSA.** We carried out EMSA and preparation of nuclear extract from Raji cells as previously described[49]. We labeled oligonucleotides −169T and −169C with digoxigenin -11-ddUTP using the DIG gel-shift kit (Roche). We incubated 5 μg of nuclear extract with 40 fmol of digoxigenin-labeled nucleotide for 25 min at room temperature. For competition experiments, we preincubated nuclear extract with unlabeled oligonucleotide (100-fold excess) before adding digoxigenin-labeled oligonucleotide. For supershift assays, we incubated 4 μg of antibodies to p50, p52, p65, RelB or cRel and rabbit IgG (control antibody; Santa Cruz Biotechnology) for 15 min at room temperature after incubation of the labeled probe. We separated protein-DNA complexes on a nondenaturing 6% polyacrylamide gel in 0.5× Tris-Borate-EDTA buffer. We transferred the gel to a nitrocellulose membrane and detected signals using an LAS-3000 lumino-image analyzer (Fujifilm).

**RNA extraction and cDNA preparation.** We collected peripheral blood from healthy volunteers to obtain $CD19^+$ lymphocytes. We separated polymorpho-nuclear cells by differential centrifugation using Lymphoprep resolving solution (AXIS-FIELD). We isolated $CD19^+$ lymphocytes using the MACS system with CD19 microbeads (Miltenyi Biotec) and confirmed that cell purity was >95% using flow cytometry. We stimulated cells with antibodies to CD40 (Cymbus Biotechnology) or IgM (Jackson Immunoresearch), with Il-4 (eBioscience), with APRIL (PeproTech), with BAFF (PeproTech) or with LPS (Sigma) for 4 h. We isolated total RNA using RNeasy Mini Kit (Qiagen). We quantified RNA in other normal tissues using Premium Total RNA (Clontech). We reverse-transcribed total RNA using TaqMan Gold RT-PCR reagents with random hexamers (Applied Biosystems) in accordance with the instructions of the manufacturer.

**Quantification of FCRL3 expression using real-time RT-PCR.** We carried out real-time quantitative PCR using an ABI PRISM 7900 (Applied Biosystems) and Assay-on-Demand TaqMan probe and primers (Hs00364720_m1 for FCRL3) in accordance with the manufacturer's instructions. We generated a standard curve from the amplification data for FCRL3 primers using a dilution series of total RNA from Raji cells as templates and normalized data to GUS level.

**ASTQ.** We carried out ASTQ as previously described[34] with some modifications. We prepared cDNA from B cells as described above. We amplified both cDNA and genomic DNA by PCR for 37 cycles using primers specific for exon 2 of FCRL3 (**Supplementary Table 4** online) and for an additional cycle using forward primer with Alexa Fluor 488 label at the 5′ end. Products were directly digested using EagI by incubation at 37 °C for 12 h. We monitored full digestion by the inclusion of PCR products from +358G/G homozygotes. We then separated digested products on a 12.5% polyacrylamide gel and quantified them using an LAS-3000 analyzer.

***In situ* hybridization and immunohistochemistry.** We carried out *in situ* hybridization as previously described[50]. We obtained probes from PCR products using the sequence of FCRL3 (nt 2052–2490, comprising the intracellular unique region that is poorly conserved among members of this family). An additional probe of the 5′ untranslated sequence yielded similar results. We also examined control probes, which yielded no specific hybridization (data not shown). We used antibodies to CD3 (clone PS-1, Nichirei) and CD20 (clone L26, Zymed) for immunohistochemistry with an ABC Elite kit (Vector Labs) in accordance with the manufacturer's instructions. No specific staining was detected using mouse isotype IgG (data not shown).

**Measurement of autoantibodies.** We measured RF in sera of individuals with rheumatoid arthritis using latex-enhanced immunonephelometric assay. We measured antibody to DNA in sera of individuals with SLE by radioimmunoassay. Individuals with rheumatoid arthritis ($n = 147$, 81.1% women; age

63.9 ± 10.6 years (mean ± s.d.); 87.8% RF-positive; mean Steinbrocker radiographic stage 3.2) or SLE ($n = 120$, 92.6% women; age 36.6 ± 12.7 years (mean ± s.d.)) were part of the cohorts or from a single medical institute, respectively. For each individual, we used the maximum value of RF and antibody to DNA measured during the treatment period in the medical center or outpatient clinic. We detected antibody to CCP at a single time point using enzyme-linked immunosorbent assay, as previously described[38].

**Statistical analysis.** We calculated LD index Δ (ref. 28) and drew **Figure 1a** using Excel software (Microsoft). We estimated haplotype frequencies using HAPLOTYPER software. We applied the $\chi^2$ test for contingency table tests for associations between allele-genotype distribution and phenotypes. FCRL3 expression in B cells and autoantibody production were regressed on the number of susceptible alleles (coded 0, 1 and 2). All other statistical analyses, unless otherwise stated, were done using STATISTICA software (StatSoft).

**URLs.** The JSNP database is available at http://snp.ims.u-tokyo.ac.jp/index.html. TRANSFAC is available at http://www.gene-regulation.com/. HAPLOTYPER is available at http://www.people.fas.harvard.edu/~junliu/Haplo/docMain.htm.

**GenBank accession number.** FCRL3 mRNA, NM_052939.

*Note: Supplementary information is available on the Nature Genetics website.*

1. Firestein, G.S. Evolving concepts of rheumatoid arthritis. *Nature* **423**, 356–361 (2003).
2. Gregersen, P.K., Silver, J. & Winchester, R.J. The shared epitope hypothesis. An approach to understanding the molecular genetics of susceptibility to rheumatoid arthritis. *Arthritis Rheum.* **30**, 1205–1213 (1987).
3. Newton, J.L., Harney, S.M., Wordsworth, B.P. & Brown, M.A. A review of the MHC genetics of rheumatoid arthritis. *Genes Immun.* **5**, 151–157 (2004).
4. Kochi, Y. *et al.* Analysis of single-nucleotide polymorphisms in Japanese rheumatoid arthritis patients shows additional susceptibility markers besides the classic shared epitope susceptibility sequences. *Arthritis Rheum.* **50**, 63–71 (2004).
5. Seldin, M.F., Amos, C.I., Ward, R. & Gregersen, P.K. The genetics revolution and the assault on rheumatoid arthritis. *Arthritis Rheum.* **42**, 1071–1079 (1999).
6. Tsao, B.P. The genetics of human systemic lupus erythematosus. *Trends Immunol.* **24**, 595–602 (2003).
7. Bowcock, A.M. & Cookson, W.O. The genetics of psoriasis, psoriatic arthritis and atopic dermatitis. *Hum. Mol. Genet.* **13** Suppl 1, R43–R55 (2004).
8. Marrack, P., Kappler, J. & Kotzin, B.L. Autoimmune disease: why and where it occurs. *Nat. Med.* **7**, 899–905 (2001).
9. Ueda, H. *et al.* Association of the T-cell regulatory gene CTLA4 with susceptibility to autoimmune disease. *Nature* **423**, 506–511 (2003).
10. Becker, K.G. *et al.* Clustering of non-major histocompatibility complex susceptibility candidate loci in human autoimmune diseases. *Proc. Natl. Acad. Sci. USA* **95**, 9979–9984 (1998).
11. Tokuhiro, S. *et al.* An intronic SNP in a RUNX1 binding site of SLC22A4, encoding an organic cation transporter, is associated with rheumatoid arthritis. *Nat. Genet.* **35**, 341–348 (2003).
12. Begovich, A.B. *et al.* A missense single-nucleotide polymorphism in a gene encoding a protein tyrosine phosphatase (PTPN22) is associated with rheumatoid arthritis. *Am. J. Hum. Genet.* **75**, 330–337 (2004).
13. Davis, R.S., Wang, Y.H., Kubagawa, H. & Cooper, M.D. Identification of a family of Fc receptor homologs with preferential B cell expression. *Proc. Natl. Acad. Sci. USA* **98**, 9772–9777 (2001).

14. Davis, R.S. *et al*. Fc receptor homologs: newest members of a remarkably diverse Fc receptor gene family. *Immunol. Rev.* **190**, 123–136 (2002).
15. Hatzivassiliou, G. *et al*. IRTA1 and IRTA2, novel immunoglobulin superfamily receptors expressed in B cells and involved in chromosome 1q21 abnormalities in B cell malignancy. *Immunity* **14**, 277–289 (2001).
16. Miller, I., Hatzivassiliou, G., Cattoretti, G., Mendelsohn, C. & Dalla-Favera, R. IRTAs: a new family of immunoglobulinlike receptors differentially expressed in B cells. *Blood* **99**, 2662–2669 (2002).
17. Xu, M.J., Zhao, R., Cao, H. & Zhao, Z.J. SPAP2, an Ig family receptor containing both ITIMs and ITAMs. *Biochem. Biophys. Res. Commun.* **293**, 1037–1046 (2002).
18. Ravetch, J.V. & Bolland, S. IgG Fc receptors. *Annu. Rev. Immunol.* **19**, 275–290 (2001).
19. Kyogoku, C. *et al*. Fcgamma receptor gene polymorphisms in Japanese patients with systemic lupus erythematosus: contribution of FCGR2B to genetic susceptibility. *Arthritis Rheum.* **46**, 1242–1254 (2002).
20. Capon, F. *et al*. Fine mapping of the PSORS4 psoriasis susceptibility region on chromosome 1q21. *J. Invest. Dermatol.* **116**, 728–730 (2001).
21. Dai, K.Z. *et al*. The T cell regulator gene SH2D2A contributes to the genetic susceptibility of multiple sclerosis. *Genes Immun.* **2**, 263–268 (2001).
22. Jirholt, J. *et al*. Genetic linkage analysis of collagen-induced arthritis in the mouse. *Eur. J. Immunol.* **28**, 3321–3328 (1998).
23. Sundvall, M. *et al*. Identification of murine loci associated with susceptibility to chronic experimental autoimmune encephalomyelitis. *Nat. Genet.* **10**, 313–317 (1995).
24. Teuscher, C. *et al*. Evidence that Tmevd2 and eae3 may represent either a common locus or members of a gene complex controlling susceptibility to immunologically mediated demyelination in mice. *J. Immunol.* **159**, 4930–4934 (1997).
25. Podolin, P.L. *et al*. Congenic mapping of the insulin-dependent diabetes (Idd) gene, Idd10, localizes two genes mediating the Idd10 effect and eliminates the candidate Fcgr1. *J. Immunol.* **159**, 1835–1843 (1997).
26. Nieto, A. *et al*. Involvement of Fcgamma receptor IIIA genotypes in susceptibility to rheumatoid arthritis. *Arthritis Rheum.* **43**, 735–739 (2000).
27. Radstake, T.R. *et al*. Role of Fcgamma receptors IIA, IIIA, and IIIB in susceptibility to rheumatoid arthritis. *J. Rheumatol.* **30**, 926–933 (2003).
28. Devlin, B. & Risch, N. A comparison of linkage disequilibrium measures for fine-scale mapping. *Genomics* **29**, 311–322 (1995).
29. Cordell, H.J. & Clayton, D.G. A unified stepwise regression procedure for evaluating the relative effects of polymorphisms within a gene using case/control or family data: application to HLA in type 1 diabetes. *Am. J. Hum. Genet.* **70**, 124–141 (2002).
30. Sebastiani, P. *et al*. Minimal haplotype tagging. *Proc. Natl. Acad. Sci. USA* **100**, 9900–9905 (2003).
31. Tsunoda, T. *et al*. Variation of gene-based SNPs and linkage disequilibrium patterns in the human genome. *Hum. Mol. Genet.* **13**, 1623–1632 (2004).
32. Pritchard, J.K., Stephens, M. & Donnelly, P. Inference of population structure using multilocus genotype data. *Genetics* **155**, 945–959 (2000).
33. Pritchard, J.K. & Rosenberg, N.A. Use of unlinked genetic markers to detect population stratification in association studies. *Am. J. Hum. Genet.* **65**, 220–228 (1999).
34. Kaijzel, E.L. *et al*. Allele-specific quantification of tumor necrosis factor alpha (TNF) transcription and the role of promoter polymorphisms in rheumatoid arthritis patients and healthy individuals. *Genes Immun.* **2**, 135–144 (2001).
35. Takemura, S. *et al*. Lymphoid neogenesis in rheumatoid synovitis. *J. Immunol.* **167**, 1072–1080 (2001).
36. Weyand, C.M. & Goronzy, J.J. Ectopic germinal center formation in rheumatoid synovitis. *Ann. N. Y. Acad. Sci.* **987**, 140–149 (2003).
37. Alarcon, G.S. *et al*. Suppression of rheumatoid factor production by methotrexate in patients with rheumatoid arthritis. Evidence•for differential influences of therapy and clinical status on IgM and IgA rheumatoid factor expression. *Arthritis Rheum.* **33**, 1156–1161 (1990).
38. Suzuki, K. *et al*. High diagnostic performance of ELISA detection of antibodies to citrullinated antigens in rheumatoid arthritis. *Scand. J. Rheumatol.* **32**, 197–204 (2003).
39. Rantapaa-Dahlqvist, S. *et al*. Antibodies against cyclic citrullinated peptide and IgA rheumatoid factor predict the development of rheumatoid arthritis. *Arthritis Rheum.* **48**, 2741–2749 (2003).
40. Capon, F., Semprini, S., Dallapiccola, B. & Novelli, G. Evidence for interaction between psoriasis-susceptibility loci on chromosomes 6p21 and 1q21. *Am. J. Hum. Genet.* **65**, 1798–1800 (1999).
41. Suzuki, A. *et al*. Functional haplotypes of PADI4, encoding citrullinating enzyme peptidylarginine deiminase 4, are associated with rheumatoid arthritis. *Nat. Genet.* **34**, 395–402 (2003).
42. Barton, A. *et al*. A functional haplotype of the PADI4 gene associated with rheumatoid arthritis in a Japanese population is not associated in a United Kingdom population. *Arthritis Rheum.* **50**, 1117–1121 (2004).
43. Jorgensen, T.N., Gubbels, M.R. & Kotzin, B.L. New insights into disease pathogenesis from mouse lupus genetics. *Curr. Opin. Immunol.* **16**, 787–793 (2004).
44. Edwards, J.C. *et al*. Efficacy of B-cell-targeted therapy with rituximab in patients with rheumatoid arthritis. *N. Engl. J. Med.* **350**, 2572–2581 (2004).
45. Gray, D. *et al*. Observations on memory B-cell development. *Semin. Immunol.* **9**, 249–254 (1997).
46. van Eijk, M., Defrance, T., Hennino, A. & de Groot, C. Death-receptor contribution to the germinal-center reaction. *Trends Immunol.* **22**, 677–682 (2001).
47. Arnett, F.C. *et al*. The American Rheumatism Association 1987 revised criteria for the classification of rheumatoid arthritis. *Arthritis Rheum.* **31**, 315–324 (1988).
48. Hochberg, M.C. Updating the American College of Rheumatology revised criteria for the classification of systemic lupus erythematosus. *Arthritis Rheum.* **40**, 1725 (1997).
49. Aikawa, Y., Yamamoto, M., Yamamoto, T., Morimoto, K. & Tanaka, K. An anti-rheumatic agent T-614 inhibits NF-kappaB activation in LPS- and TNF-alpha-stimulated THP-1 cells without interfering with IkappaBalpha degradation. *Inflamm. Res.* **51**, 188–194 (2002).
50. Hoshino, M. *et al*. Identification of the stef gene that encodes a novel guanine nucleotide exchange factor specific for Rac1. *J. Biol. Chem.* **274**, 17837–17844 (1999).

# Localization of peptidylarginine deiminase 4 (PADI4) and citrullinated protein in synovial tissue of rheumatoid arthritis

X. Chang[1], R. Yamada[1], A. Suzuki[1], T. Sawada[2], S. Yoshino[3], S. Tokuhiro[1] and K. Yamamoto[1,2]

*Objectives.* Peptidylarginine deiminases (PADIs) convert peptidylarginine into citrulline via post-translational modification. Anti-citrullinated peptide antibodies are highly specific for rheumatoid arthritis (RA). Our genome-wide case−control study of single-nucleotide polymorphisms found that the PADI4 gene polymorphism is closely associated with RA. Here, we localized the expression of PADI4 and the citrullinated protein product in synovial RA tissue.

*Methods.* We used immunohistochemistry, double immunofluorescent labelling and western blotting.

*Results.* We found that PADI4 is extensively expressed in T cells, B cells, macrophages, neutrophils, fibroblast-like cells and endothelial cells in the lining and sublining areas of the RA synovium. We also found extracellular and intracellular expression of PADI4 in fibrin deposits with loose tissue structures where apoptosis was widespread. Unlike PADI4, citrullinated protein generally appeared in fibrin deposits that were abundant in the RA synovium. The citrullinated fibrin aggregate was immunoreactive against immunoglobulin (Ig) A and IgM, but not IgG and IgE. Although a little PADI4 was expressed in osteoarthritic and normal synovial tissues, significant citrullination was undetectable.

*Conclusions.* The results showed that PADI4 is mainly distributed in cells of various haematopoietic lineages and expressed at high levels in the inflamed RA synovium. The co-localization of PADI4, citrullinated protein and apoptotic cells in fibrin deposits suggests that PADI4 is responsible for fibrin citrullination and is involved in apoptosis. The immunoreactivity of citrullinated fibrin with IgA and IgM in the RA synovium supports the notion that citrullinated fibrin is a potential antigen of RA autoimmunity.

KEY WORDS: Rheumatoid arthritis, Peptidylarginine deiminase 4 (PADI4). Citrullination. Fibrin, Synovial tissue.

Rheumatoid arthritis (RA) is a widespread autoimmune disease that is characterized by chronic joint inflammation. Serum from patients with RA contains diverse autoantibodies that constitute one primary outcome of disturbed immunoregulation [1]. In addition to rheumatoid factor (RF), anti-filaggrin autoantibody (AFA), anti-keratin antibody (AKA), anti-perinuclear factor (APF) and anti-cyclic citrullinated peptide antibody (anti-CCP) are highly specific for RA [2–6]. Recent studies indicate that the primary constituent of the B-cell epitope for AFA, AKA, APF and anti-CCP is citrulline, an amino acid metabolite of arginine [7–9]. Because of the specific anti-citrullinated protein antibodies in patients with RA, understanding protein citrullination, the enzymatic conversion of arginine to citrulline, should provide novel insights into RA pathogenesis.

Peptidylarginine deiminases (PADI) post-translationally modify peptidylarginine to citrulline in the presence of calcium ions and can change the conformation and functional properties of target proteins after citrullination [10]. To date, PADI1, PADI2, PADI3 and PADI4 have been identified in the human genome and all of them cluster on chromosome 1p36, a candidate region for RA susceptibility [11–13]. Our large-scale genome-wide case−control study using single-nucleotide polymorphisms found that a PADI4 polymorphism is distinctly associated with RA [14].

PADI4 was originally cloned from human myeloid leukaemia HL-60 cells that were exposed to the granulocyte-inducing agent retinoic acid, dimethyl sulphoxide, or the monocyte-inducing agent 1α,25-dihydroxyvitamin D3. The 2238 base pairs of PADI4 cDNA encode 663 amino acids that have 50–55% sequence identity with the other three known PADIs [15]. Immunohistochemical studies have detected PADI4 in neutrophils and eosinophils of human peripheral blood [16–18]. To understand its role in RA pathogenesis, we investigated the expression of PADI4 and the citrullinated protein in human synovial tissues and peripheral blood using immunohistochemical means. We also discuss here the possible pathway of PADI4 involvement in RA autoimmunity.

## Methods and materials

### Anti-PADI4 antibody preparation

We raised antisera against human PADI4 by immunizing rabbits with a synthetic oligopeptide (PAKKKSTGSSTWP, the amino acid sequence specific for the N-terminal of PADI4). The antibody was purified by affinity chromatography through a column containing histone-tagged recombinant PADI4.

[1]Laboratory for Rheumatic Diseases, SNP Research Center, Institute of Physical and Chemical Research (RIKEN), Kanagawa, [2]Department of Allergy and Rheumatology, Graduate School of Medicine, University of Tokyo and [3]Department of Joint Disease and Rheumatism, Nippon Medical School, Tokyo, Japan.
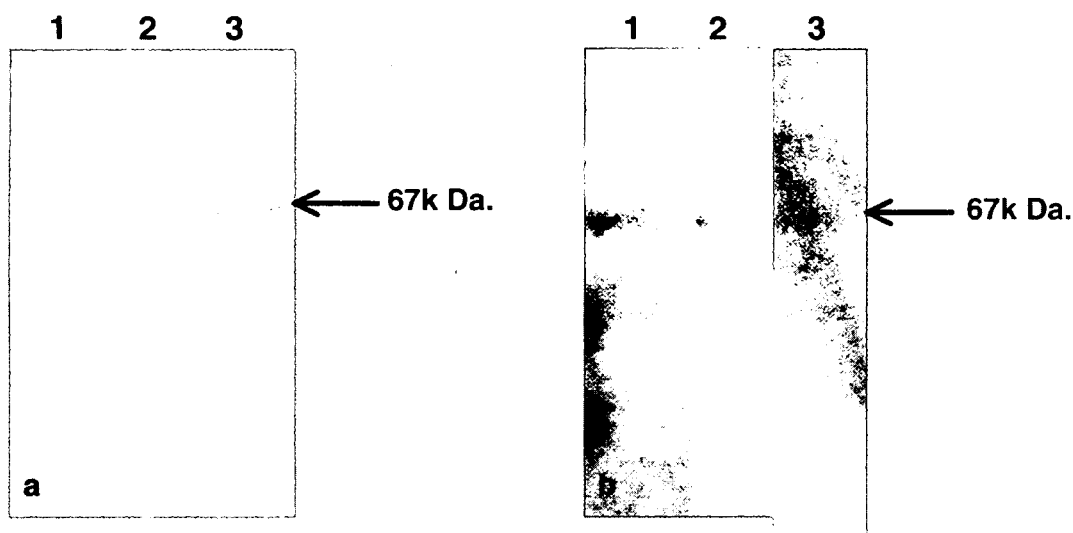
**40**

FIG. 1. PADI4 expression determined by western blotting. (a) Cultured HEK293 cells were transfected with expression vector containing coding regions of PADI4 or PADI2 or without inserts. Western blotting with anti-PADI4 antibody detected a 67-kDa band in extracts of cells expressing PADI4 (lane 3). No signals were detected in cells transfected with vector alone (lane 1) or with vector expressing PADI2 (lane 2). (b) Total proteins were extracted from RA synovial tissue (lane 1), leucocyte fraction of peripheral blood from healthy individuals (lane 2) and liver (lane 3). Western blotting shows 67-kDa PADI4 products in synovial samples but not liver samples.

## Preparation of peripheral blood

Leucocytes were separated using Monopoly Resolving Medium (DaiNippon) according to the manufacturer's instructions, from samples of fresh blood obtained from 10 RA patients and nine healthy volunteers. The cells were fixed in 4% paraformaldehyde for 2 h at room temperature and then sedimented by centrifugation. Cell pellets were resuspended in phosphate-buffered saline (PBS) and spotted onto Superfrost/Plus microscope slides (Fisher).

## Sample preparation of synovial and other tissues

We obtained written informed consent to collect synovial tissue samples from 12 patients with RA and five with osteoarthritis (OA) during arthroplasty. The tissues were fixed in 10% neutral buffered formalin (Sigma) for 12 h at room temperature, embedded in paraffin and sectioned by standard procedures. We also used Tissue Microarray Human Synovitis (Biocat), which includes 14 RA, 12 OA and four normal synovial tissue specimens for comparison. All RA patients met the American College of Rheumatoid Arthritis revised criteria for RA.

We determined the specificity of the PADI4 rabbit antibody and the tissue distribution of PADI4 using Vastarray (InnoGenex), a commercial tissue array slide containing normal human liver, lung, kidney, skin, muscle, brain thymus, spleen, lymph node and tonsil tissues.

## Immunohistochemistry

Tissue sections were deparaffinized and rehydrated using standard procedures. Slides spotted with blood cells were processed in the same manner except for deparaffinization.

To increase immunostaining intensity, the sections were heated at 95°C for 20 min with DAKO Target Retrieval Solution (Dako). Sections were incubated with first antibody overnight at 4°C, washed three times, each for 5 min, with PBS, and then incubated with SimpleStain MAX-AP Multi (Nichirei) for 30 min at room temperature. Immunoreactive signals were visualized using the

New Fuchsin Substrate kit (Nichirei) according to the manufacturer's instructions and the cell structure was defined by counterstaining with haematoxylin.

Rabbit polyclonal anti-citrulline antibody (Upstate), monoclonal anti-human fibrin (Monosan), monoclonal anti-human immunoglobulin (Ig) G Fc region, monoclonal anti-human IgM Fc region, monoclonal anti-human IgA heavy chain and monoclonal anti-human IgE Fc region (all from Zymed) were obtained commercially.

Before applying the anti-citrulline antibody, tissue sections were treated using the modification buffer supplied with the kit and then incubated with the first antibody according to the manufacturer's instructions.

## Double immunofluorescent immunohistochemistry

The tissue sections were processed as described above. Monoclonal antibodies for various cell surface CD markers (CD3, CD15, CD20, CD34 or CD68) (Zymed), fibroblast-like cell marker [proxylyl 4-hydroxylase $\beta$ (ph$\beta$)] (Daiichi Fine Chemicals) or Igs (IgG, IgM, IgA or IgM) (Zymed) were incubated together with rabbit antibody against PADI4 or citrulline at 4°C for 12 h. After three 5-min washes with PBS, sections were incubated with the secondary antibody for 30 min at room temperature. The monoclonal antibody and rabbit antiserum were detected using fluorescein isothiocyanate-goat anti-mouse IgG (H+L) conjugate (Zymed) and Cy™ 5-goat anti-rabbit IgG (H+L) conjugate (Zymed), respectively. Immunofluorescent signals were examined using a confocal microscope (Leica). CD3^{+} characterized T cells, CD20^{+} B cells, CD15^{+} neutrophils and CD68^{+} monocytes in peripheral blood or macrophages in tissues. CD34^{+} identified endothelial cells or their precursors in new capillaries.

## Detection of apoptosis

We detected apoptotic cells by immunohistochemistry and double immunofluorescent labelling as described above, together with use of the monoclonal antibody M30CytoDeath (Roche). This antibody can recognize a specific caspase cleavage site within
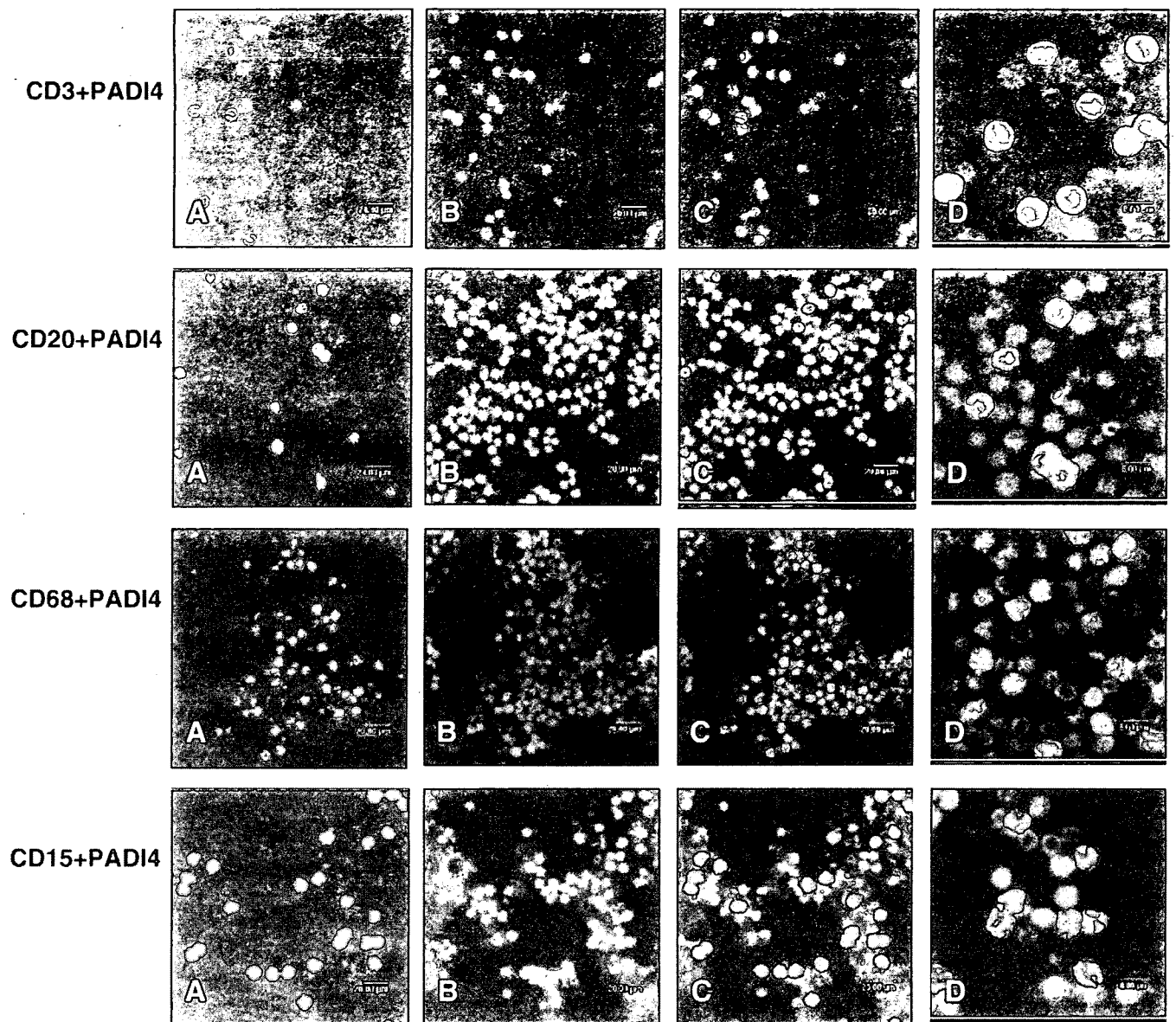
FIG. 2. Immunostaining of PADI4 in peripheral leucocytes. Peripheral leucocytes from healthy individuals were incubated with monoclonal antibodies against various cell surface CD marker and anti-PADI4 antibody. All CD-marked cells (green in A) expressed PADI4 (red in B). C, merged image of A and B; D, magnification of C. Yellow colour in merged images indicates co-localization of two protein targets. Scale bar, 20 μm in A, B and C and 8 μm in D.

cytokeratin 18 (CK18) that is not present in the native CK18 of normal cells. During the very early stage of apoptosis, caspases cleave CK18, an acidic cytokeratin intermediate filament protein of 45 kDa. The ApopDETEK Assay System (Enzo) was used to localize apoptotic cells by labelling fragmented DNA with biotinylated 16dUTP using terminal deoxynucleotide transferase. Biotinylated DNA was then visualized using the Horseradish Peroxidase-DAB *in situ* Detection System (Enzo).

*Western blotting*

Cultured HEK293 cells were transfected with the pTargetT™ mammalian expression vector (Promega) containing the complete PADI4 or PADI2 cDNA coding region. After a 60-h incubation, crude cellular protein was extracted by standard ultrasonic

disruption. The total protein of transfected cells was separated by sodium dodecyl sulphate–polyacrylamide gel electrophoresis, transblotted onto nylon membranes and probed with anti-PADI4 antibody. A western blotting kit (KPL) was used to detect signals according to the manufacturer's instructions.

To investigate PADI4 expression in synovial tissue and peripheral leucocytes, we purified total protein of RA synovial tissues and leucocytes using total protein extraction kits (Biochain). Leucocytes were prepared using Monopoly Resolving Medium as described above. The blotted membrane was probed using our anti-PADI4 antibody and the western blot kit. The total protein in a commercial liver sample served as the control (Biochain).

Written consents was obtained from all patients and healthy volunteers according to the Declaration of Helsinki. The design of the work has been approved by the ethical committees of the
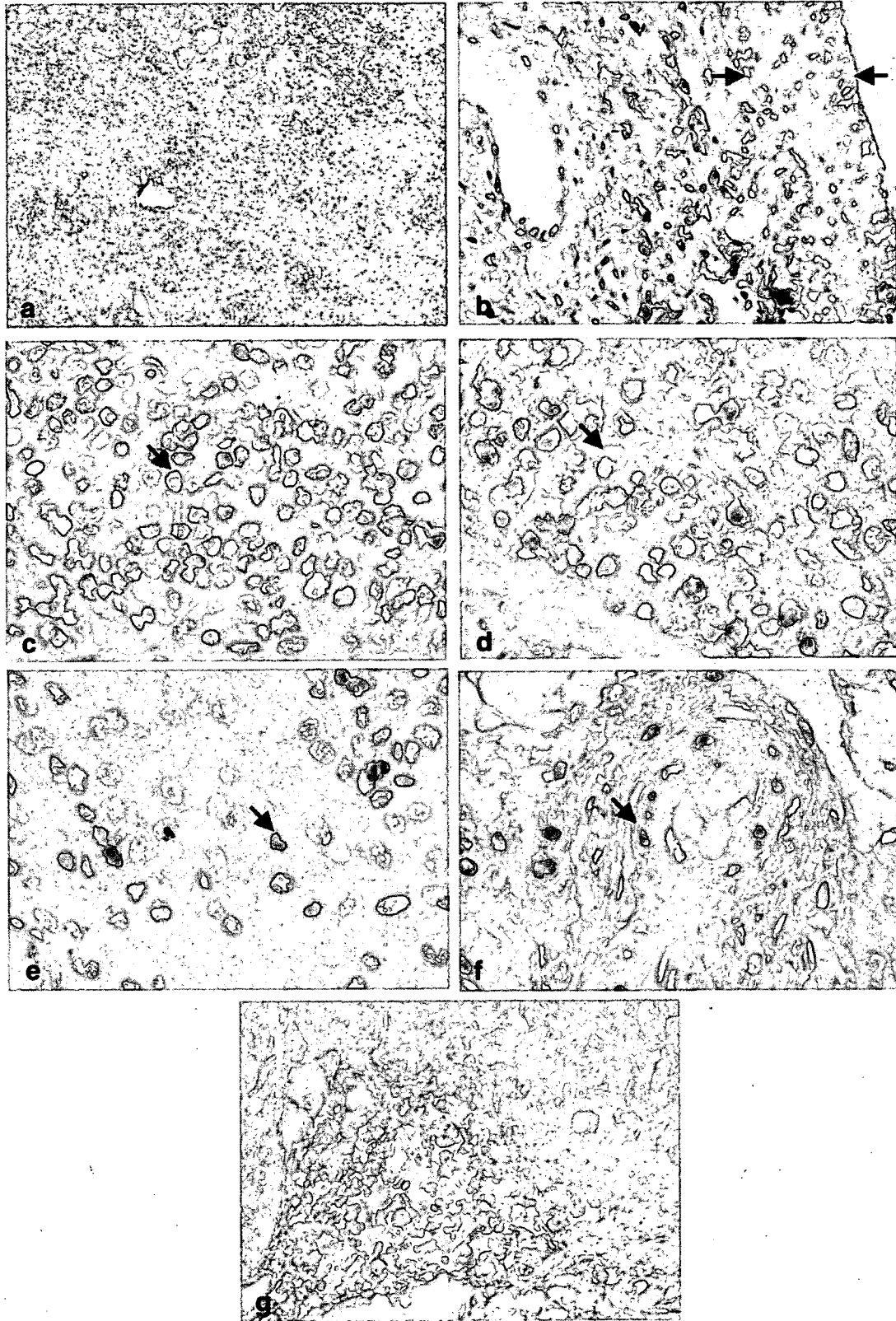
Fig. 3. Immunostaining of PADI4 in synovial RA tissue. (a) Extensive distribution of PADI4 in synovial RA tissue. (b) PADI4 is significantly expressed in the lining area marked with arrows. (c, d, e and f) Expression of PADI4 in potential lymphocytes, macrophages, polymorphic nuclear cells and capillary endothelial cells, respectively (arrows). (g) Intracellular and extracellular expression of PADI4 in loose tissue that was usually close to solid fibrin deposits and which contained cells with apoptotic morphology. Original magnification: a, 40×; b, 200×; c, d, e and f, 400×.
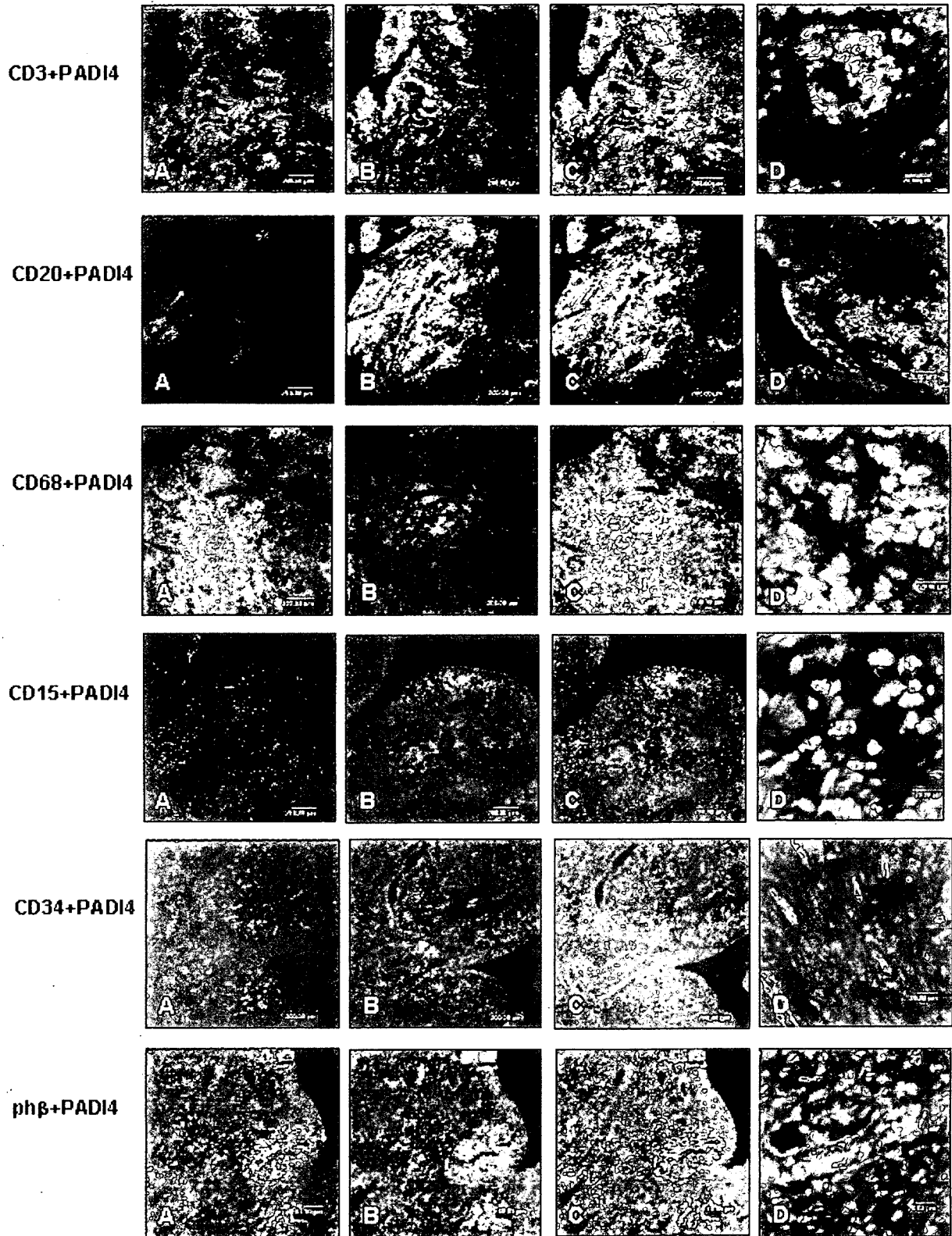
FIG. 4. Cellular distribution of PADI4 in RA synovial tissue. Synovial RA membrane was incubated with anti-PADI4 and monoclonal antibodies against leucocyte cell surface CD markers or phβ. All CD3-, CD20-, CD68-, CD15- and phβ-marked cells (green in A) expressed PADI4 (red in B). C is a merged image of A and B. D is magnification of C image. Yellow colour in merged images indicates co-localization of two protein targets. Scale bar, 200 μm in A, B and C, 20 μm in D.
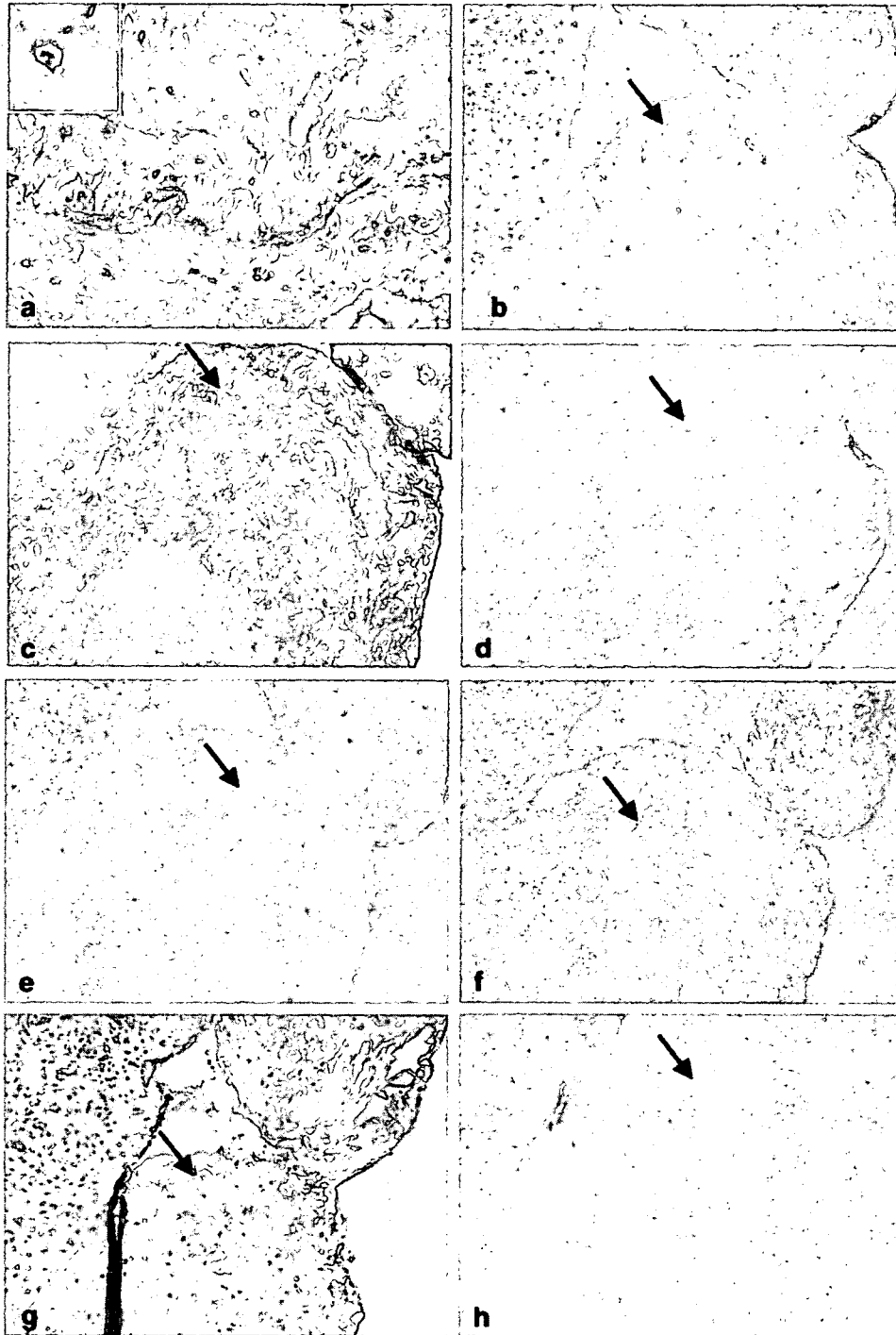
Fig. 5. Immunostaining of fibrin, citrullinated protein, PADI4, IgG, IgM, IgA and IgE in RA synovial tissue. (a) Citrullinated protein is located in some RA synovial cells in the sublining. The left upper corner is a partial magnification, indicating intracellular localization of citrullinated proteins. (b) Fibrin deposit with solid structure. (c) Citrullinated protein is located in the solid fibrin region in a continuous section. PADI4 (d) and IgG (e) were undetectable in the fibrin block. (f) Part of a solid fibrin deposit is lightly stained with anti-IgM antibody. (g) Citrullinated fibrin block was stained intensely with antibody against IgA. Capillary endothelial cells are also immunoreactive to antibody. (h) IgE was undetectable in synovial tissue. Significant IgG (i) and Ig M (j) deposits are obvious in synovial cells in the sublining of the same tissue. Arrow indicates a solid fibrin block. Original magnification: a, 400×: all other sections, 100×. (b), (c), (d), (e), (f), (g) and (h) are continuous sections. The image at the corner is shown at partial magnification.
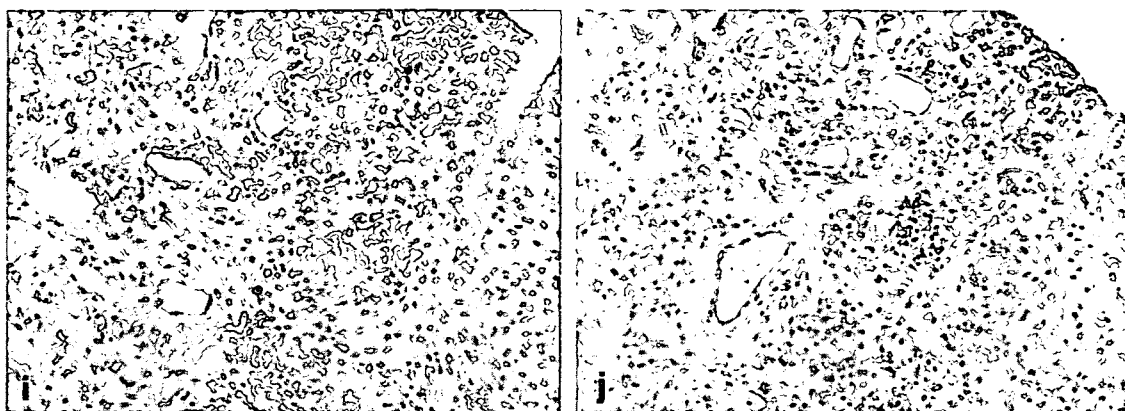
i
j

FIG. 5. Continued.

Institute of Physical and Chemical Research (RIKEN) and conforms to standards currently applied in Japan.

## Results

### *Western blotting with PADI4 antibody*

The anti-PADI4 antibody detected a band of 67 kDa in lysates of cultured HEK293 cells transfected with PADI4 expression vectors, but not in cells transfected with PADI2 or blank vector (Fig. 1a). Using the same antibody, western blotting detected a 67-kDa band in total proteins extracted from RA synovial tissue and in peripheral leucocytes of both RA patients and healthy individuals, but not in the liver of the healthy individuals (Fig. 1b). These results confirmed the specificity of our anti-PADI4 antibody. Some groups have identified a similarly sized PADI4 product in stimulated HL60 cells and in isolated synovial macrophages using an antibody against recombinant PADI4 protein [15–19].

### *Immunohistochemistry of PADI4 in peripheral blood cells*

Double immunofluorescent labelling using anti-PADI4 antibody and antibodies against various cell surface CD markers showed that all $CD3^+$ T, $CD20^+$ B cells and $CD15^+$ granulocytes of peripheral blood expressed nuclear PADI4. $CD68^+$ monocytes also expressed nuclear and cytoplasmic PADI4 (Fig. 2). No differences were evident between samples of blood from patients with RA and healthy controls. The antibody against citrullinated protein did not detect any signals in peripheral leucocytes (data not shown).

### *Immunohistochemistry of PADI4 in RA synovial tissue*

Immunohistochemistry with the anti-PADI4 antibody showed a broad distribution of PADI4 in many types of cells in RA synovial tissue (Fig. 3a). The lining consisted of abundant hyperplastic cells that stained intensely for PADI4 (Fig. 3b). Small mononuclear cells with little cytoplasm formed many clusters of nodular infiltrates. The nuclei of these cells were significantly stained with anti-PADI4 antibody, particularly at the nuclear edge (Fig. 3c). Large mononuclear cells with abundant cytoplasm predominated in RA synovial tissue. These macrophage-like and fibroblast-like cells were clustered in the lining and sublining of RA synovial tissue, or were dispersed in regions with a loose tissue structure. Both the cytoplasm and nuclei of these cells expressed high levels of PADI4 (Fig. 3d). In addition, polymorphonuclear cells that were evenly distributed throughout the sublining distinctly expressed nuclear PADI4 (Fig. 3e). Extensive angiogenesis is a primary feature of RA synovial tissue. The nuclei of endothelial cells surrounding small capillaries obviously expressed PADI4 peptide (Fig. 3f). PADI4 was also expressed intracellularly and extracellularly in loosely organized tissue in which the cells showed the morphology of apoptosis, having condensed chromatin, cytosol vacuolization and being separated from surrounding tissue [20] (Fig. 3g).

We investigated which type of cells contained PADI4 by double immunofluorescent labelling using an antibody for PADI4 and various CD cell markers (Fig. 4). Both $CD3^+$ T cells and $CD20^+$ B cells surrounding small capillaries expressed nuclear PADI4. The cytoplasm and nuclei of $CD68^+$ macrophages, which constitute one of the key structural components of the inflamed RA synovial membrane, expressed PADI4. $CD15^+$ cells were evenly distributed in the tissue and their polymorphic nuclei expressed PADI4. We identified angiogenic regions by detecting $CD34^+$ cells that were functional endothelial cells or the active precursors of new capillaries. The nuclei of all $CD34^+$ cells in the RA synovium were significantly immunostained with anti-PADI4 antibody. Besides, fibroblast-like cells marked with ph$\beta$ antibody also expressed PADI4. The double immunofluorescent staining results were consistent with those of standard immunohistochemistry. The results were identical in all 12 of our RA samples and in 14 commercially available RA specimens.

Anti-fibrin antibody identified a significant amount of fibrin deposition in RA synovial tissues. Based on our observations, most of these fibrin deposits formed a solid block and some fibrin appeared as a mesh or spongy structure with loosely organized cells (Figs 5b and 6a). The spongiform structure, which was usually located close to the solid fibrin block, expressed large amounts of intracellular and extracellular PADI4 protein (Fig. 6c).

### *Immunohistochemistry of citrullinated peptides in RA synovial tissue*

We immunolocalized citrullinated protein in the RA synovium using a polyclonal antibody against citrullinated peptide. Unlike the extensive distribution of PADI4, only a few synovial cells were immunostained in the sublining of the tissue (Fig. 5a). Citrullinated protein was primarily located in the solid fibrin block, which was not stained by anti-PADI4 antibody (Fig. 5b–d).

We investigated the deposition of IgG, IgM, IgA and IgE, which are central components of the autoimmune reaction, in continuous sections. Although IgG and IgM were highly immunoreactive in numerous cells at the sublining of the tissue (Fig. 5i and j), only a little fibrin deposit was mildly stained with the antibody against IgM (Fig. 5e and f). However, the citrullinated fibrin blocks in 80% of tested samples stained intensely with the antibody against IgA (Fig. 5g). IgA

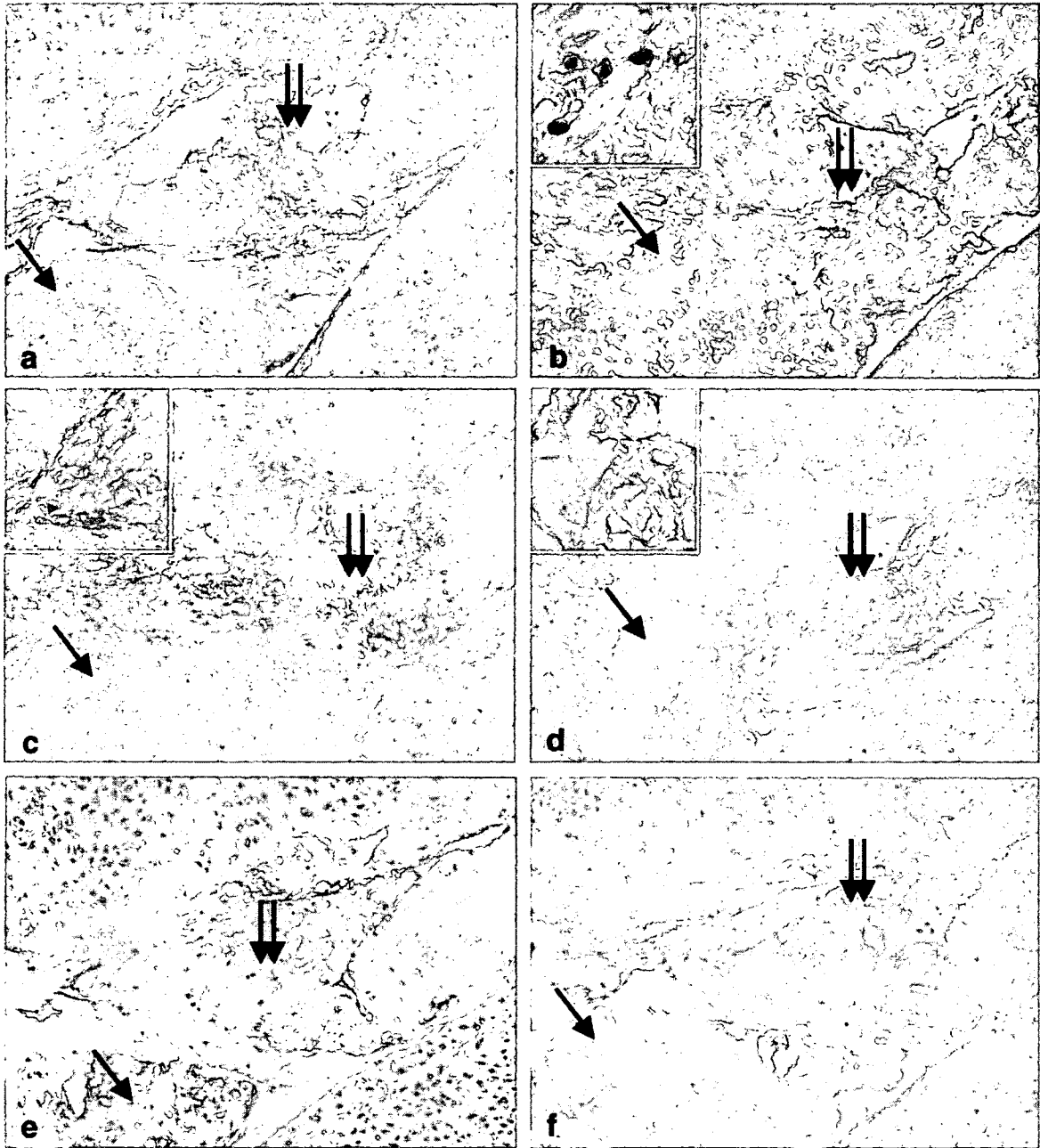



FIG. 6. Immunostaining of citrullinated protein, PADI4, apoptosis, IgG, IgM, IgA and IgE in fibrin deposits in continuous sections of RA synovial tissue. (a) A cell-loose region of RA synovial tissue was immunostained with anti-fibrin antibody. (b) Citrullinated protein is present in both solid (single arrows) and spongy (double arrows) fibrin deposits on continuous sections. (c) PADI4, (d) M30CytoDeath and fragmented DNA (e) are exclusively localized in meshed fibrin deposit. No immunosignals of IgG (f), IgM (g) and IgE (h) were evident in fibrin deposits. (i) The area of fibrin deposits is highly immunoreactive for IgA. (original magnification: (a–i), 100×). The inset images are shown at partial magnification.

immunoreaction was also detected in endothelial cells around small capillaries. The RA synovium did not express IgE immunoreactivity (Fig. 5h). These results were reproducible using anti-Ig antibodies from another manufacturer (Biomeda).

Spongiform masses that consisted of about 10% fibrin expressed intracellular citrullinated protein (Fig. 6a and b) that co-localized with PADI4 and apoptotic cells (Fig. 6c–e). Double immunofluorescent labelling also confirmed the co-localization of apoptotic cells and citrullinated protein in some fibrin deposits (results not shown). Most apoptotic cells were localized in the spongiform

fibrin mass with loosely organized cells. Like the solid form, the fibrin mesh was significantly stained with antibody against IgA rather than IgG, IgM or IgE (Fig. 6f–i).

*Immunohistochemistry of PADI4 in OA synovial membrane and other tissues*

Immunohistochemistry using antibodies against various types of leucocytes and fibrin indicated that OA synovial tissue contains
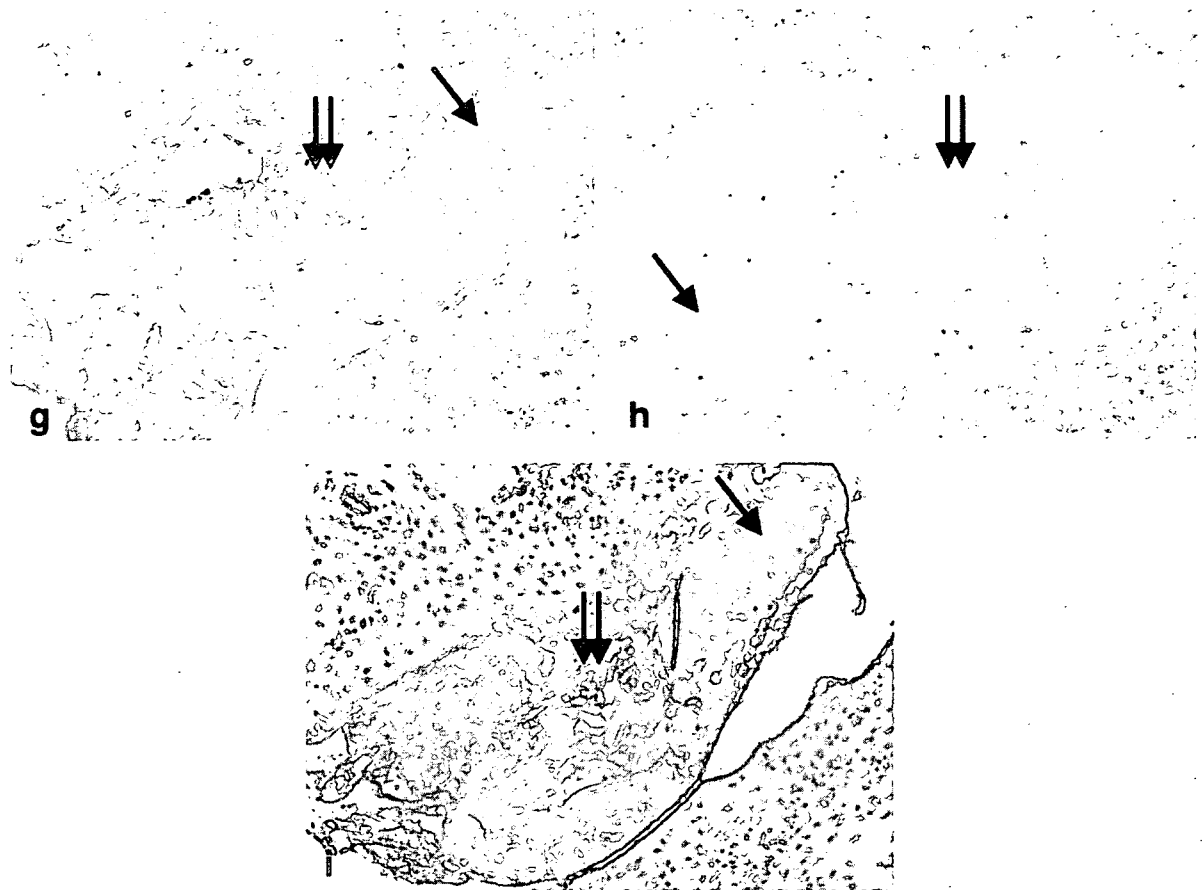
FIG. 6. Continued.

a few CD68$^+$ macrophages but lacks lymphocyte infiltrate, a hyperplastic structure and fibrin deposits. Macrophages of OA synovial tissue expressed low levels of PADI4 (Fig. 7a). Because PADI4 is mainly expressed in lymphocytes and macrophages, the loose cell structure and absence of lymphocyte infiltrate contributed to the low density of PADI4 immunostaining in OA synovial tissue. Like the findings in peripheral blood, citrullination was insignificant in OA synovial tissue (Fig. 7b). The results were similar in all 12 OA samples and in four commercially available specimens from healthy individuals.

Immunohistochemistry using the human tissue array showed distinct PADI4 expression in some regions of haematopoietic tissues, including the thymus, spleen and tonsils. The expression of PADI4 was not evident in over 30 other human tissues, including the lungs, stomach, kidneys, liver and brain (results not shown), although capillary endothelial cells and some stroma cells of these organs were stained with the anti-PADI4 antibody. Because the brain, skin and muscle express high levels of PADI1, PADI2 or PADI3 [13], the absence of immunostaining of PADI4 in these tissues further confirmed the specificity of our anti-PADI4 antibody.

In all the above experiments, no immunosignals were detected in the negative controls, which included samples with normal serum instead of the first antibody, as well as those without first or second antibodies.

## Discussion

The present study provides evidence that PADI4 is expressed in peripheral blood CD3$^+$ T cells, CD20$^+$ B cells, CD15$^+$ neutrophils

and CD68$^+$ monocytes. We also identified PADI4 in the same subtypes of leucocytes, fibroblast-like cells and capillary endothelial cells in RA synovial tissue. Screening over 30 normal human tissues showed selective PADI4 expression in haematopoietic tissues, including the thymus, spleen and bone marrow. Thus, we suggest that the cells expressing PADI4 in the RA synovium are mainly limited to haematopoietic cells or their derivatives. We previously detected PADI4 transcripts by northern hybridization only in haematopoietic tissues, including the spleen, thymus, peripheral blood leucocytes, fetal liver and bone marrow [14]. Mouse and rat PAD4, a homologue of human PADI4, is also expressed at high levels in granulocytes and monocytes [13, 21].

The expression of PADI4 did not differ in peripheral leucocytes from RA patients and healthy individuals. Vossenaar *et al.* also obtained similar results by reverse transcription–polymerase chain reaction and immunoblotting [19]. Moreover, we did not detect citrulline production in blood cells. These findings imply that the expression of PADI4 and its citrullination activity in the synovium both play critical roles in the pathogenesis of RA. The inflamed RA synovial membrane is formed mainly through the abnormal proliferation of macrophages and fibroblast-like cells, as well as by excessive infiltration of lymphocytes from the circulation [22]. These types of cells constitute the main source of PADI4 expression according to the present results and other studies [13, 14, 19]. Therefore, we observed extensive PADI4 expression in RA rather than OA synovial tissue or normal synovium. Vossenaar *et al.* also suggested that inflamed RA joints contain high levels of PADI peptide [19]. In addition, they localized PADI4 mRNA only in monocytes and showed that the PADI4 transcript degrades after the cells differentiate into synovial macrophages,